Cambridge Centre for Computational Chemical Engineering

University of Cambridge

Department of Chemical Engineering

Preprint ISSN 1473 – 4273

Analyzing the limits of a stable Homogeneous Charge Compression Ignition (HCCI) operation

Amit Bhave, Markus Kraft [1], Aaron Oakley, Hua Zhao [2],

Fabian Mauss [3]

submitted: 5th August 2004

[1] Department of Chemical Engineering
University of Cambridge
Pembroke Street
Cambridge CB2 3RA
UK
E-Mail: markus_kraft@cheng.cam.ac.uk

[2] Department of Mechanical Engineering
Brunel University
Uxbridge
Middlesex UB8 3PH
UK

[3] Division of Combustion Physics
Lund Institute of Technology
Box 118, S-221 00 Lund
Sweden

Preprint No. 24

c4e

Key words and phrases. HCCI, operating window, misfire.

Edited by
Cambridge Centre for Computational Chemical Engineering
Department of Chemical Engineering
University of Cambridge
Cambridge CB2 3RA
United Kingdom.

Fax: + 44 (0)1223 334796
E-Mail: c4e@cheng.cam.ac.uk
World Wide Web: http://www.cheng.cam.ac.uk/c4e/

Abstract

We present a computational tool to develop an operating window for a homogeneous charge compression ignition (HCCI) engine. A single cylinder Ricardo E-6 engine running in HCCI mode with external exhaust gas recirculation (EGR) is being simulated using an improved probability density function (PDF) based engine cycle model. For a base case, the in-cylinder temperature and unburned hydrocarbon emissions predicted by the model show a satisfactory agreement with measurements [Oakley et al., SAE Paper 2001-01-3606]. Furthermore, the integrated model is applied to develop the engine operating window for various combustion parameters, emissions and engine parameters with respect to the air-fuel ratio and the amount of EGR used. The model predictions agree reasonably well with the experimental results for various parameters over the entire operating range thus proving the robustness of the PDF based model. The boundaries of the operating window namely, knocking, partial burn, and misfire are reliably predicted by the model. In particular, the model provides a useful insight into the misfire phenomenon by depicting the cyclic variation in the ignition timing and in-cylinder pressure profiles. Finally, we investigate two control options, namely heating intake charge and trapping residual burnt fraction by negative valve overlap. The effect of these two methods on HCCI combustion and CO, HC and NO_x emissions is studied.

Contents

1 Introduction

Homogeneous Charge Compression Ignition (HCCI), an advanced mode of engine operation is attractive on account of its efficiency as high as the conventional modes of internal combustion engine operation, low NO_x emissions, and virtually no particulate matter (PM) emissions. Commercializing HCCI technology, however, remains a formidable challenge due to its narrow operating regime and intrinsic difficulties in controlling combustion phasing.

An operating window describes the limits of a stable engine operation for a range of operating conditions. Early use of operating maps for HCCI was presented by Thring (1989). In that study the operating regime of a single cylinder four-stroke HCCI engine was mapped as a function of equivalence ratio and EGR rates. Drawbacks of HCCI in terms of a small operating window and difficulty in controlling the auto-ignition were pointed out. Later, Smith et al. (1997) used the homogeneous reactor model to map the operation of a methane fuelled HCCI engine. The region of acceptable HCCI operation was depicted by plotting various parameters such as indicated efficiency, burn duration, NO emissions and ignition timing with respect to the residual burnt fractions and air-fuel ratios. The limits of the maps were given by partial burn, region of fast combustion, and a region of early combustion. The transition between partial burn and complete burn was found to be extremely sharp. In case of two-stroke HCCI operation, Gentili and Frigo (2000) plotted a load-speed operating field while demonstrating direct high pressure liquid injection HCCI operation for the first time. On comparing the operating fields for three injection methods, namely: direct high pressure liquid injection, indirect (premixed) injection and air-assisted injection, the first one was found to exhibit the widest operating range. Oakley et al. (2001) established the operating range of HCCI engine with regard to air-fuel ratio and EGR. Taking a similar approach to Thring (1989), a range of stable HCCI operation was identified for various fuels such as alcohols, and blends of gasoline, while maintaining constant inlet temperature and compression ratio. A large difference in the tolerance to dilution existed between the various fuels studied. The range of possible, naturally aspirated HCCI engine operation has been scanned by Koopmans and Denbratt (2001). Three valve timing events were used to cover the complete range of the unthrottled HCCI engine. Three zones that limit the stable HCCI operation were identified on a load-speed map. Zone 1 given by high cycle to cycle variation at low-load and low-speed, zone 2 representing knocking and zone 3 with high speeds and low loads giving misfire. Zhao et al. (2002) operated a four-stroke multi-cylinder engine in HCCI mode with a stoichiometric air-fuel ratio without intake charge heating or higher compression ratios, by trapping large amount of residual burnt gases. Their load-speed operating map showed a stable HCCI operation between load range, 0.5 to 4 brake mean effective pressure (BMEP) and speed range 1000 to 3500 RPM. In the load-speed range investigated, knocking was not observed but the two main limits of the stable operation were identified. For high loads, at each speed, maximizing the airflow resulted in maximum possible BMEP. At each load there was a minimum BMEP

which was limited by misfire. Lately, for miniature HCCI engines operational maps have been presented by Aichlmayr et al. (2002) using the homogeneous modelling approach. Based on the mappings, they pointed out that the extent of the engine operational space can be increased at the expense of a reduction in power density.

Computational modelling provides a time and cost effective mean to develop such operating windows and evaluate strategies to expand them. Probability density function (PDF) based closed volume (Bhave et al.; 2004a) as well as engine cycle (Bhave et al.; 2004b) models have been successfully applied for modelling HCCI operation. These models include detailed chemical kinetics and do not face reaction rate closure problems. Furthermore, the models account for turbulent mixing, fluid-wall interactions and fluctuations, inherent to an engine operation.

In this paper, the PDF based engine cycle model has been applied to develop an operating window for various combustion parameters, emissions, and engine parameters with respect to the amount of EGR and air-fuel ratio. In addition to the narrow operating window, challenges in controlling HCCI operation need to be overcome. In the second part of the paper, two distinct approaches adopted to overcome the HCCI control hurdle are investigated:

1. Increasing the inlet charge temperature by incorporating a heater in the engine cycle.

2. Trapping of residual burned fraction using variable valve actuation with standard compression ratios.

2 Engine description

In this section, the geometry and the operating parameters of the Ricardo E-6 engine (Figure 1) are discussed. This is followed by the description of the experimental procedures adopted for the measurements and construction of the operating window. This explanation is included here to complement the simulation procedure explained in the next section. All the experimental results were taken from Oakley et al. (2001). The specifications of the four-stroke Ricardo engine are given in Table 1. The compression ratio for the engine was variable in the range 4.5:1 to 18:1 using a worm gear, able to control the height of cylinder head relative to the crankshaft. It was measured with a calibrated micrometer mounted at the side of the cylinder and was fixed at 11.5:1 for the present study. The valve timings given in Table 1 yielded a valve overlap period of around 14° around TDC on the induction stroke and prevented exhaust back-flow when the intake manifold pressure is low relative to the exhaust. The engine was fuelled with PRF-95, i.e., a mixture of 95% iso-octane and 5% n-heptane, by volume.

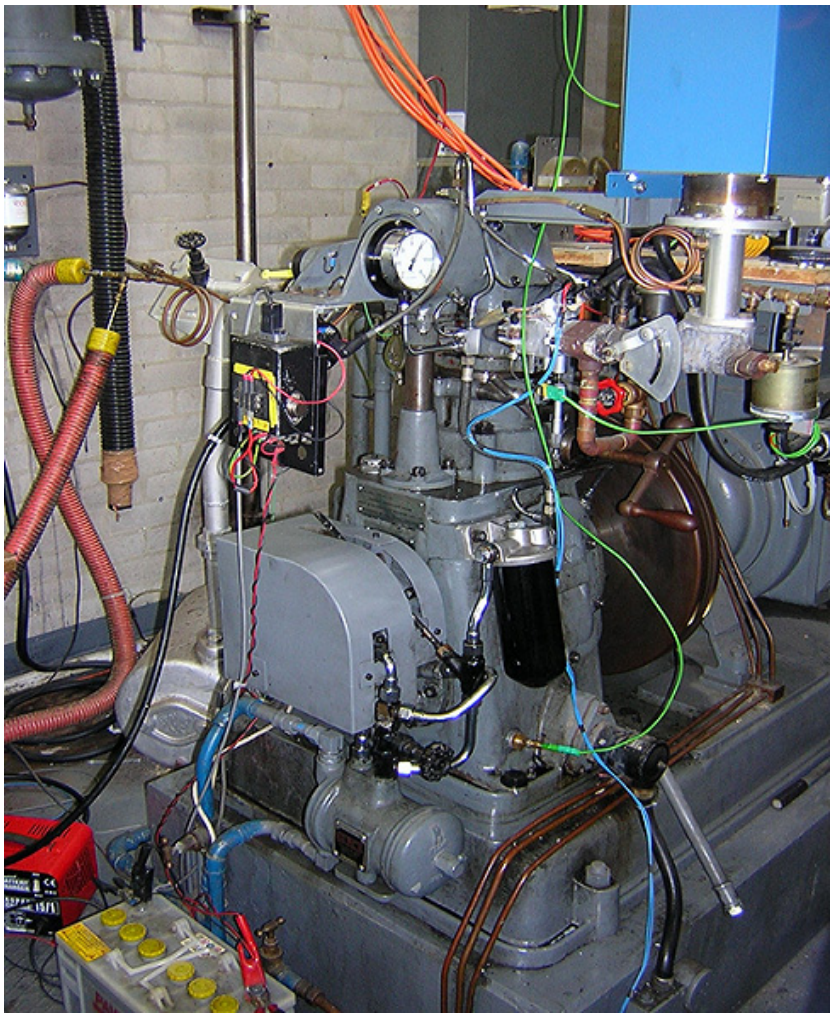

Figure 1: *Ricardo E-6 engine converted to HCCI mode.*

Table 1: *Ricardo E-6 engine geometry and operating parameters.*

Description	**Value**
Displaced Volume	504 cm^3
Bore	76.2 mm
Stroke	111.1 mm
Exhaust Valve Open	43° BBDC (at 5 mm lift)
Exhaust Valve Close	6° ATDC (at 5 mm lift)
Inlet Valve Open	8° BTDC (at 5 mm lift)
Inlet Valve Close	36° ABDC (at 5 mm lift)
Speed	1500 RPM
Fuel	PRF-95
Compression ratio	11.5

The experimental set-up is shown in Figure 2. Air was mixed with the EGR (when the EGR valve was open), and passed through a 3 kW intake gas heater. The heated gas was then passed through the manually controlled throttle. A port fuel injector directed towards the intake valve was mounted.

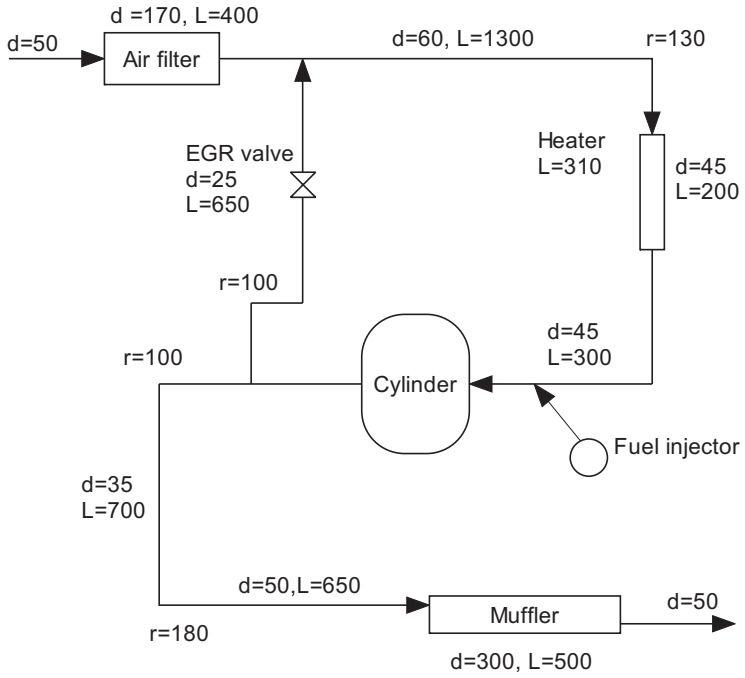

Figure 2: *Experimental set-up of the Ricardo E-6 engine.*

The exhaust gases were split into two streams. The main stream passed through the gate valve used to control the exhaust back-pressure, to the exhaust measurement unit. The second stream passed through the EGR valve and mixed with the fresh air stream to form an almost homogeneous air-EGR mixture.

A water-cooled piezoelectric type pressure transducer, capable of measuring gauge pressures in the range 0-100 bar was used in the engine block. For the measurement and control of the intake and exhaust gas temperatures as well as the coolant and oil temperatures, thermocouples were employed at various locations around the engine. A non-dispersive infrared absorption cell was employed to measure CO, CO_2 and O_2. The NO_x emissions were analyzed using a chemiluminescent NO_x analyzer. The exhaust unburned hydrocarbon concentrations were measured using the flame ionization detection technique.

3 Model description

An improved PDF based full cycle model was employed to simulate the combustion, emissions and the gas exchange processes in the HCCI engine. The integrated

model comprises of the PDF based stochastic reactor model coupled with a 1-D engine cycle simulator. The model has been explained in detail in the previous work (Bhave et al.; 2004b). The engine mapped on the 1-D code interface is shown in Figure 3. For the present engine with EGR, 49 uncoupled cycles (1-D code only) were found to be necessary to stabilize the mass flow rates on the basis of the flow through the EGR valve. This was followed by 4 homogeneous reactor model based coupled cycles and 2 PDF model based coupled cycles. The first PDF based coupled cycle was performed with 50 stochastic particles and the second with 100 particles. The total computational time for one complete simulation with 55 cycles was 17 h. While providing the temperature at IVC, the 1-D code accounts for the residual burnt fraction, EGR and fresh charge. This temperature was assigned to all the stochastic particles as the initial condition. Similarly, the composition of each stochastic particle in the ensemble is same at IVC. The chemical mechanism for the primary reference fuel contained 157 species and 1552 chemical reactions (Bhave et al.; 2004b).

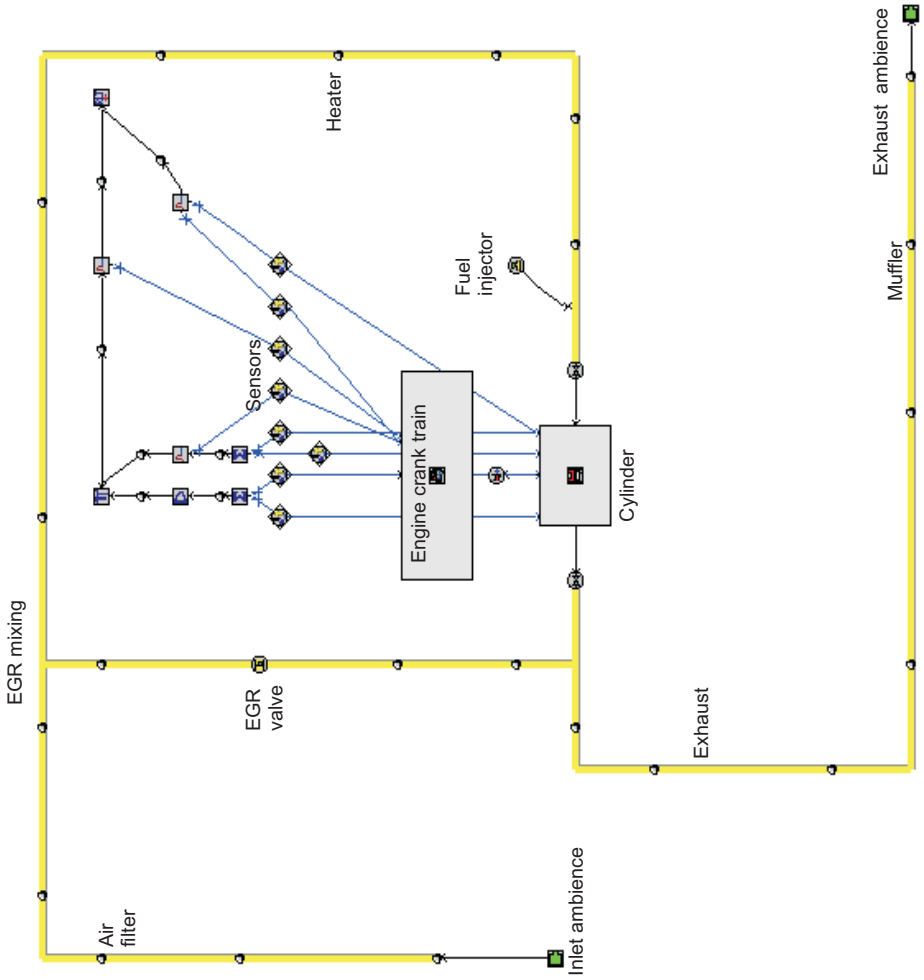

Figure 3: *Ricardo E-6 engine mapped using the 1-D code.*

4 Model validation

Before constructing the operating window for the present engine, the model was calibrated by comparing the in-cylinder temperature and emissions with the measurements for a base case. The engine operating conditions are as given in Table 1 and the model parameters are given in Table 2.

Table 2: *Model input parameters*

T_w (K)	C_h	τ (s)	T_{IVC} (K)	Fuel mass (mg/cycle)
450	40.0	0.02	493	7.5

T_W stands for the wall temperature whereas C_h denotes the constant of fluctuation and τ the characteristic turbulent mixing time. For these conditions the in-cylinder temperature profile and the unburned HC emissions measured by Oakley (2001) were compared to the model predictions shown in Figure 4.

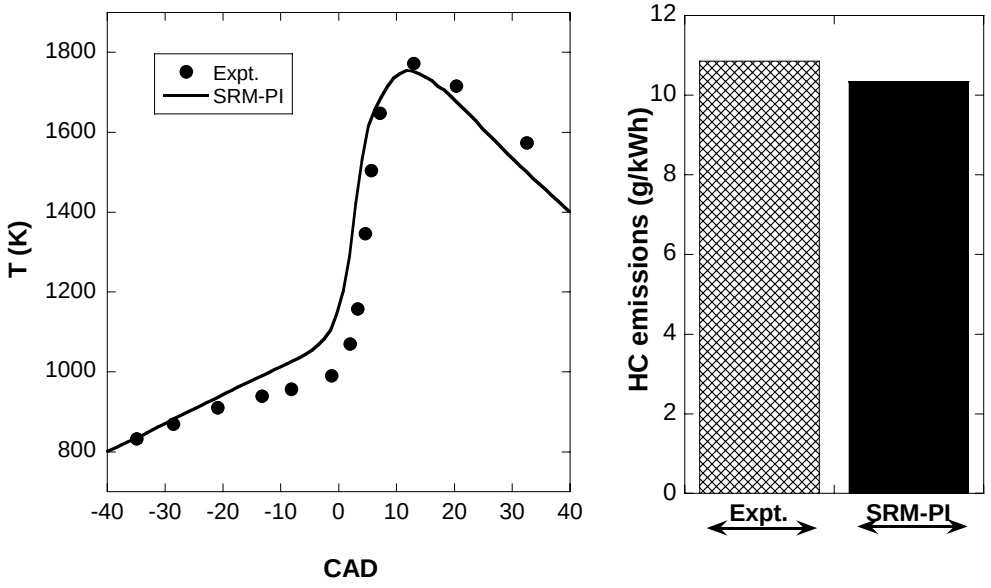

Figure 4: *In-cylinder temperature and HC emissions: Comparison of SRM-PI predictions with measurements.*

The comparison of the model predictions with measurements showed a good agreement for the in-cylinder temperature profile. The auto-ignition timing and the peak temperature were predicted well, however the temperature at auto-ignition was over-predicted as compared to that in the measurements. This can be attributed to the activity of low temperature chemistry in the chemical mechanism. The comparison

of the experimental and predicted values of HC emissions suggested a reliable HC prediction. Having validated the model, the parameters namely, T_W, C_h and τ used in Table 2 were kept constant throughout the present work. The model was then applied to map the operating window for the HCCI engine as described in the next section.

5 Operating window

In the present work, the integrated full cycle model was run for 23 points (each point corresponding to a specific air-fuel ratio and EGR) as shown in Figure 5. The total computational time for these 23 points was around 14 days on an Athlon XP2000, 1.67 GHz PC. Interpolation was used to develop the contour plots for various parameters such as indicated mean effective pressure (IMEP), combustion duration, temperature at IVC, indicated thermal efficiency as well as the CO, HC, and NO_x emissions with respect to the air-fuel ratio and the amount of EGR. The contour plots for the predicted quantities were compared with measurements. Thus, such a comparison provided a rigorous validation of the model calculations.

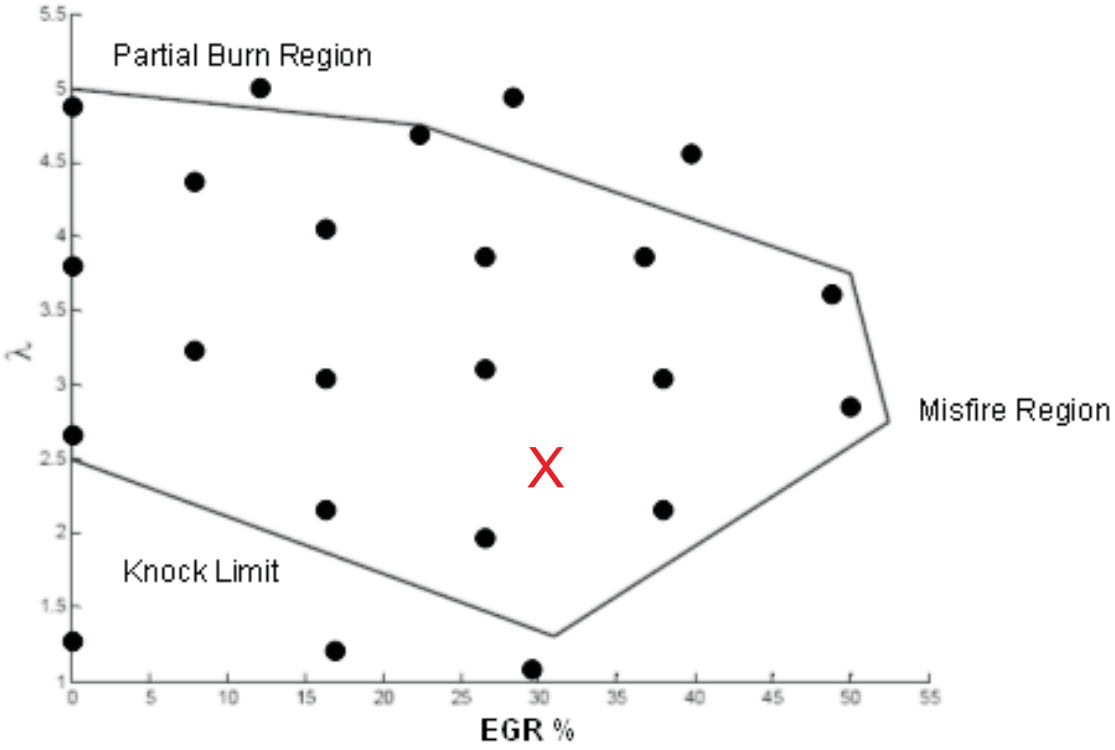

Figure 5: *Operating window: Data points for SRM-PI model.*

The operating window depicted in Figure 5 is bounded by three regions, namely: partial burn, misfire, and knock. Knock occurs when an excessively violent rise in

heat release causes pressure fluctuations. Partial burn occurs when the air-fuel ratio is too lean to allow the full oxidation of the fuel. Misfire occurs when an intolerable amount of exhaust gases are recycled back into the cylinder, causing some of the engine cycles to fail to ignite. The cycle-to-cycle variation due to this effect is further aggravated by the lean air-fuel ratios. In the experiments, the misfire condition was quantified as the point at which more than 1% of the cycles failed to burn. The base case used for validation in the previous section is denoted by the cross at a point corresponding to $\lambda = 2.5$ and 32% EGR.

Figures 6 to 14 depict the comparison of the model predictions and measurements for various parameters over the entire operating range.

The IMEP prediction (Figure 6(a)) and the measurements (Figure 6(b)) showed a good agreement. Higher loads were obtained nearer to the knock boundary, as the air-fuel ratio becomes richer. The highest attainable load predicted by the model was 3.5 bar (93% of the experimental value). With increasing air dilution, low loads were achieved. At such low loads, partial burning set in with a loss in combustion efficiency and rise in fuel consumption. The model successfully predicted the partial burn boundary on the basis of two factors; very high CO and HC emissions, and zero IMEP (for points lying in the partial burn region in Figure 5).

The rate of in-cylinder pressure rise is an important parameter to identify the onset of knock. From Figure 7, it was observed that the isolines run parallel to the knock boundary. Thus the rate of pressure rise shows a qualitatively similar dependence on air and EGR dilution. For the points lying in the knock region of Figure 5, an excessively high rate of pressure rise is predicted. The value is approximately 20 bar/CAD and indicates onset of knock in agreement with the results elsewhere (Chen et al.; 2001; Oakley; 2001; Christensen; 2002).

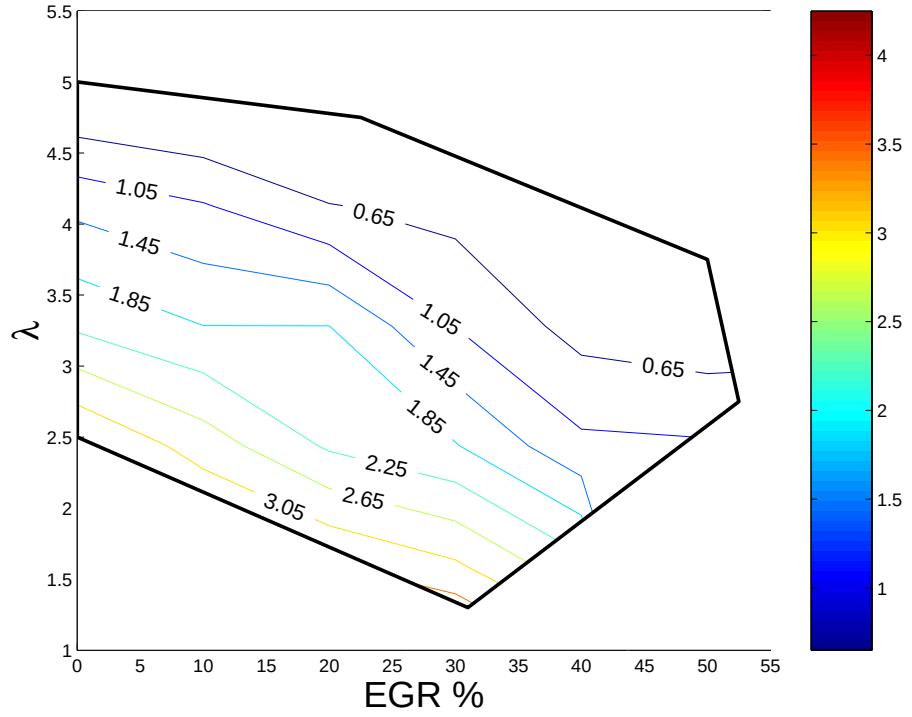

(a) IMEP range prediction

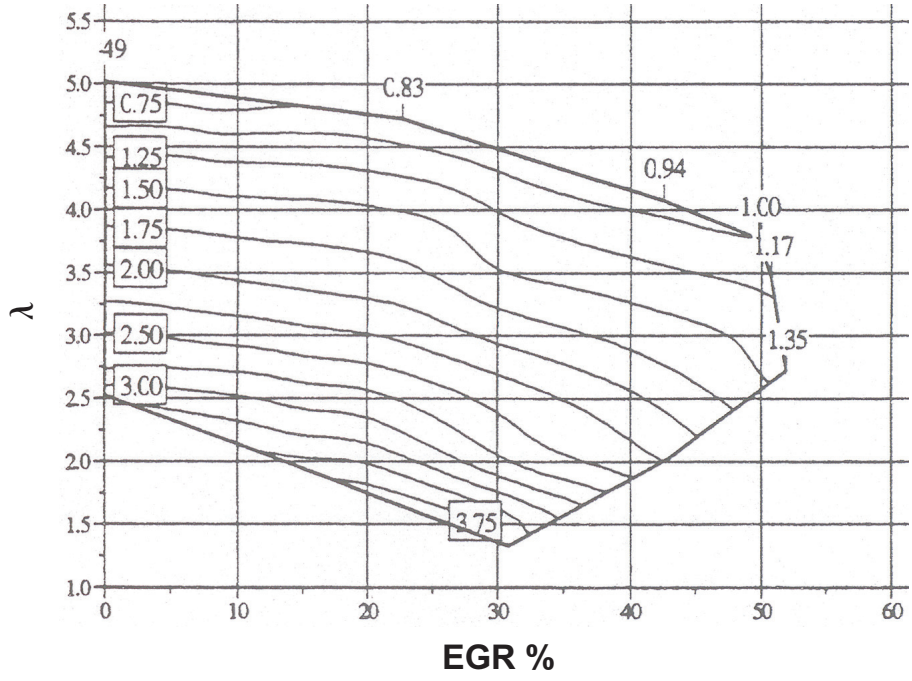

(b) IMEP range measurements

Figure 6: *IMEP (bar) as a function of air/fuel ratio and EGR.*

The temperature at IVC (Figure 8) and the exhaust gas temperature (Figure 9) were reported in °C for the experimental results (Oakley; 2001). To facilitate comparison, the model predictions for these two parameters are also given in the same units.

In the experimental set-up the temperature at IVC as shown in the Figure 8(b) was maintained in the range of 200 °C to 220 °C over the operating range. In the model set-up, the heater temperature was adjusted such that the temperature was maintained in the experimental range as shown in Figure 8(a).

The model predictions (Figure 9(a)) and the experimental results (Figure 9(b)) for exhaust gas temperature denote the highest values as conditions approached stoichiometric air/fuel ratio, and the lowest values with high air dilution. Over the entire operating range the exhaust gas temperature was predicted well.

Indicated thermal efficiency and indicated specific fuel consumption are generally used to express the efficiency of an engine. The former dimensionless parameter is preferred over the latter when comparing a range of fuels on the same engine. Figure 10 shows the operating maps for indicated thermal efficiency obtained from both model predictions and measurements. Similar to the IMEP behaviour, the richer the air-fuel mixture the greater the efficiency. With air dilution, the efficiency is reduced. The maximum and minimum efficiency values were predicted reliably compared to those obtained from measurements.

Combustion duration is calculated as the CAD difference between 10% and 90% mass fraction burnt. With a rapid rate of combustion near the knock boundary, the combustion duration was about 6 CAD. The combustion duration increased with high dilution rates for air as well as EGR as shown in Figure 11. The convergence of the predicted isolines occurred near the misfire boundary (Figure 11(a)). However, the isolines observed in the measurements (Figure 11(b)) converged more densely at the misfire boundary near the stoichiometric air/fuel ratio. The uncertainty related to the experimental evaluation of the mass fraction burnt and the averaging of combustion duration over the cycles are possible sources of this discrepancy.

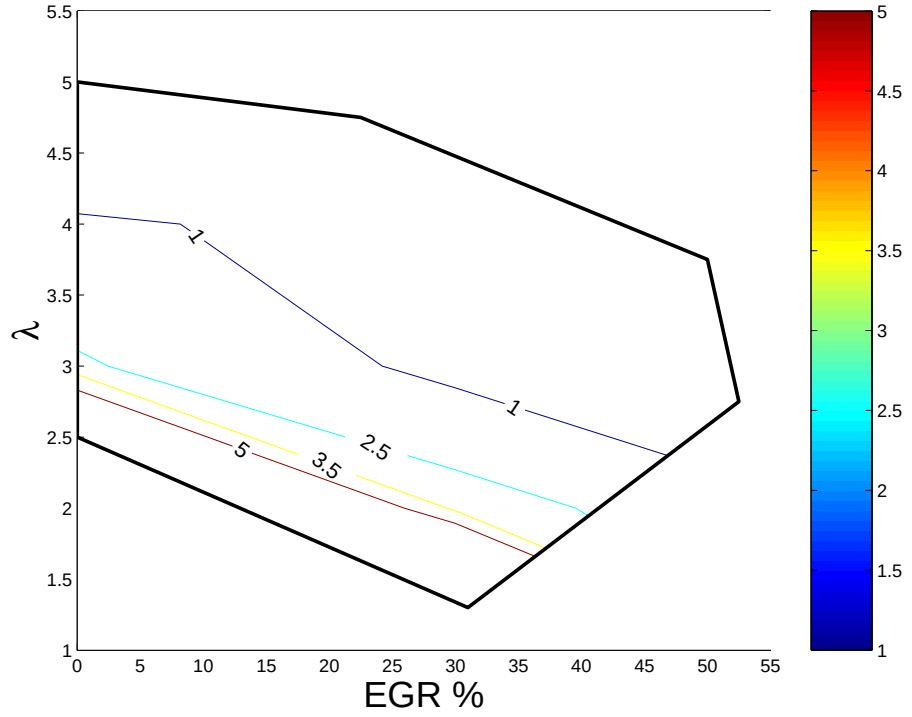

(a) Maximum rate of pressure rise prediction

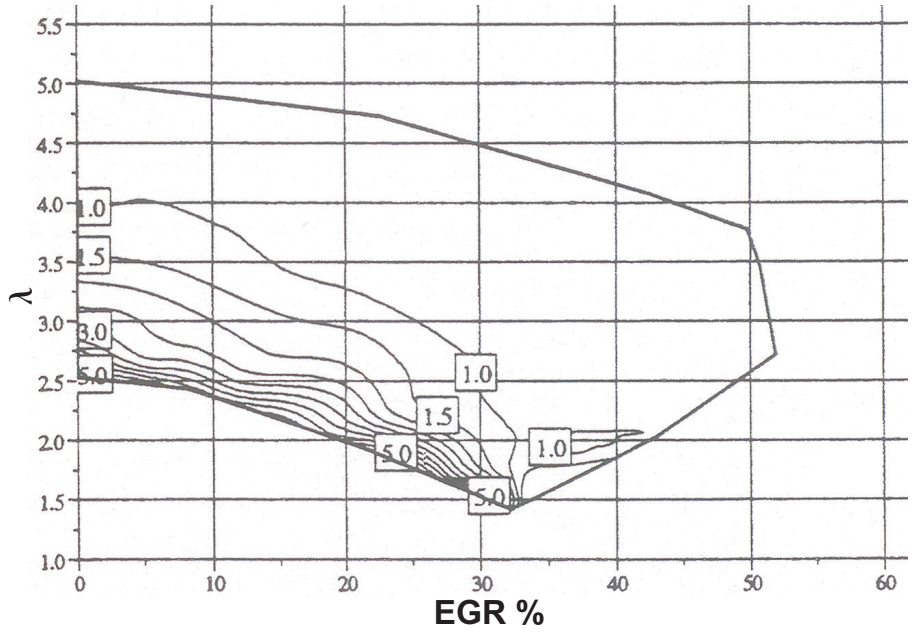

(b) Maximum rate of pressure rise measurements

Figure 7: *Maximum rate of pressure rise (bar/CAD) as a function of air/fuel ratio and EGR.*

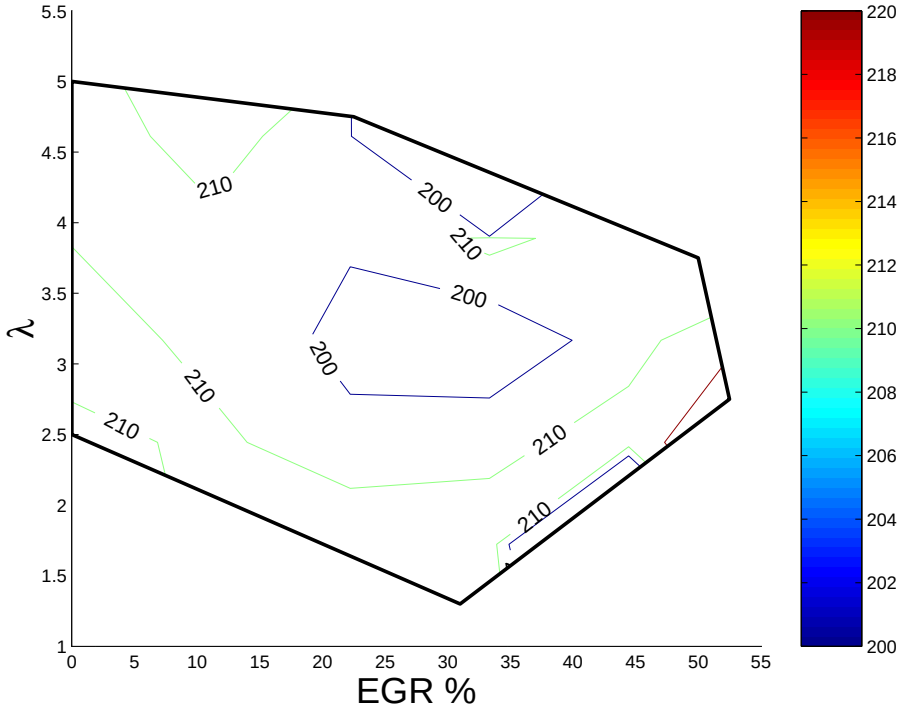

(a) Inlet gas temperature prediction

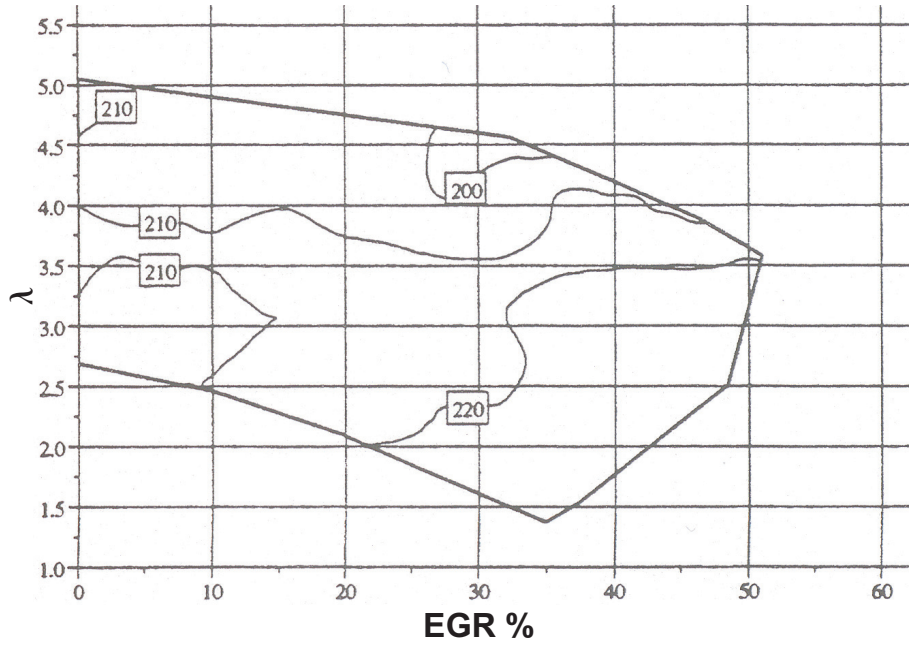

(b) Inlet gas temperature measurements

Figure 8: *Inlet gas temperature (°C) as a function of air/fuel ratio and EGR.*

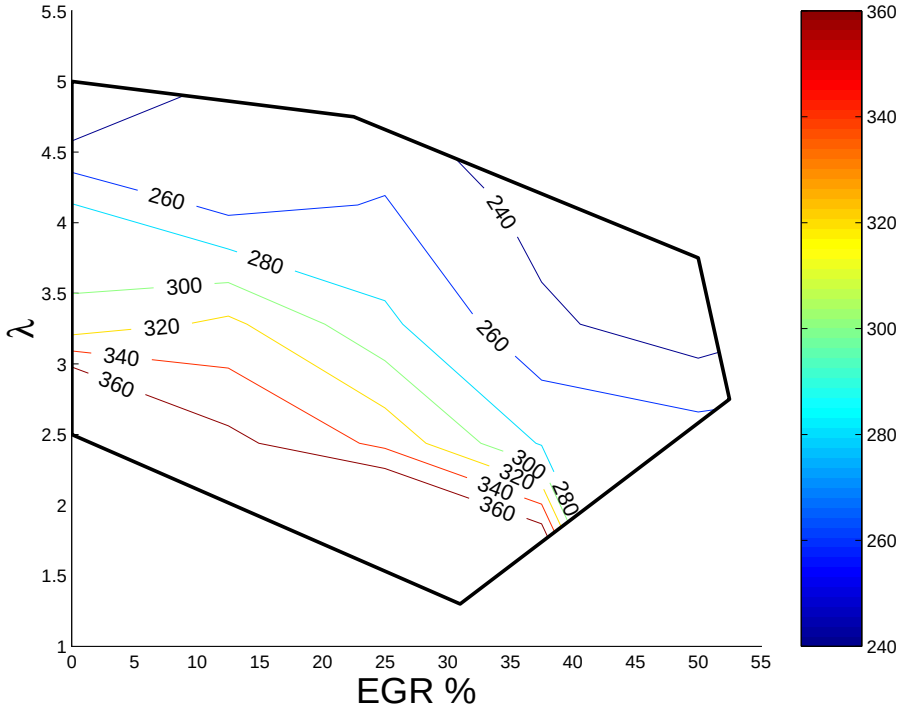

(a) Exhaust gas temperature prediction

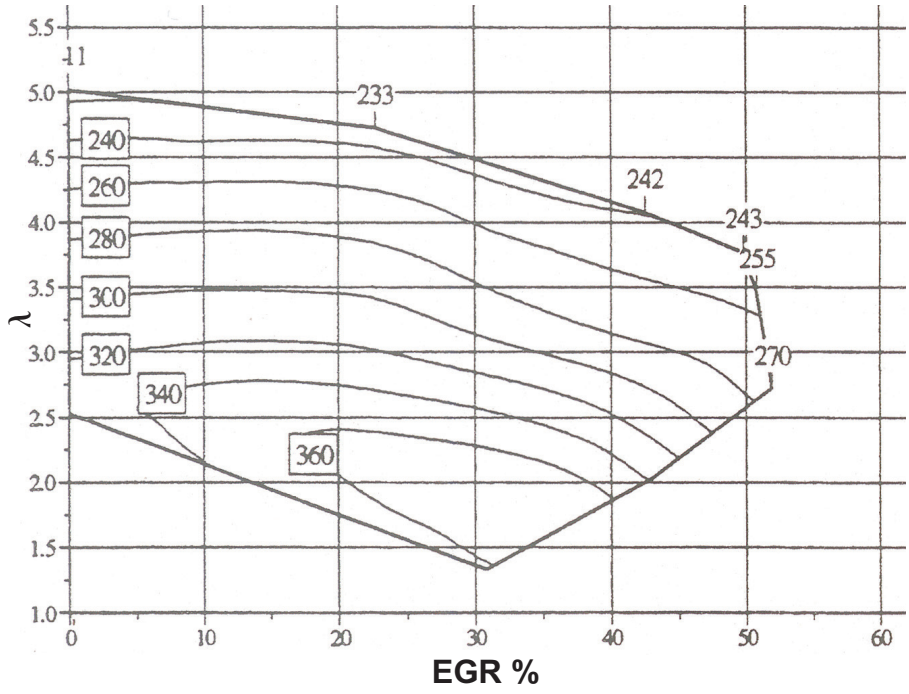

(b) Exhaust gas temperature measurements

Figure 9: *Exhaust gas temperature (°C) as a function of air/fuel ratio and EGR.*

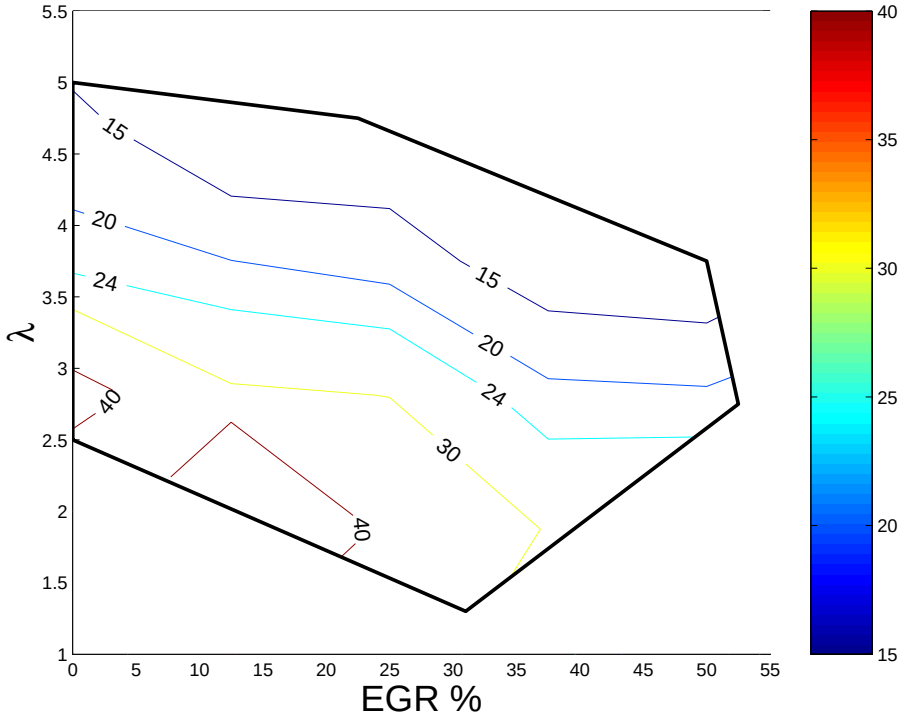

(a) Indicated thermal efficiency prediction

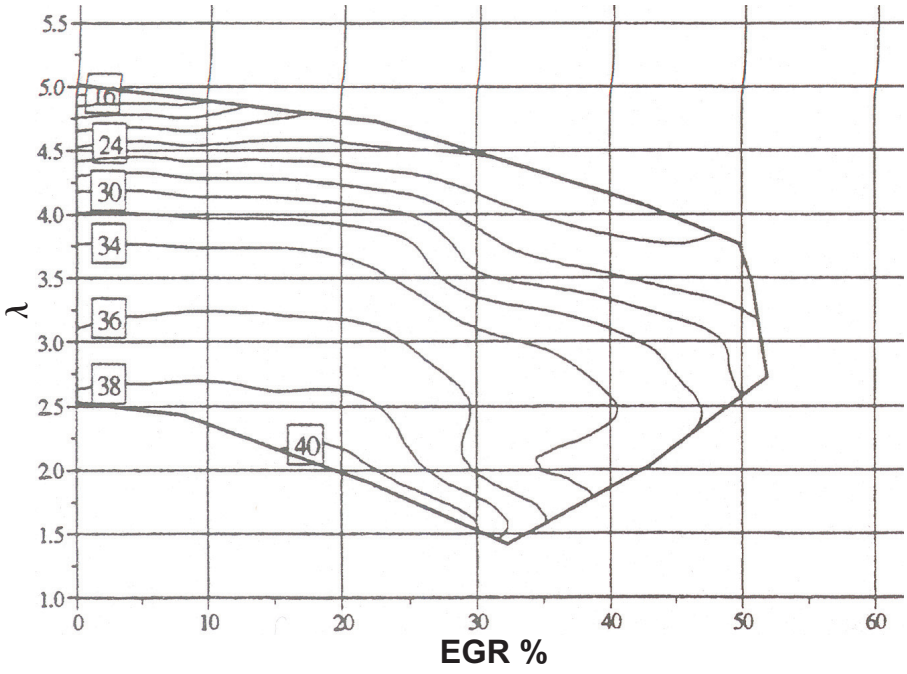

(b) Indicated thermal efficiency measurements

Figure 10: *Indicated thermal efficiency as a function of air/fuel ratio and EGR.*

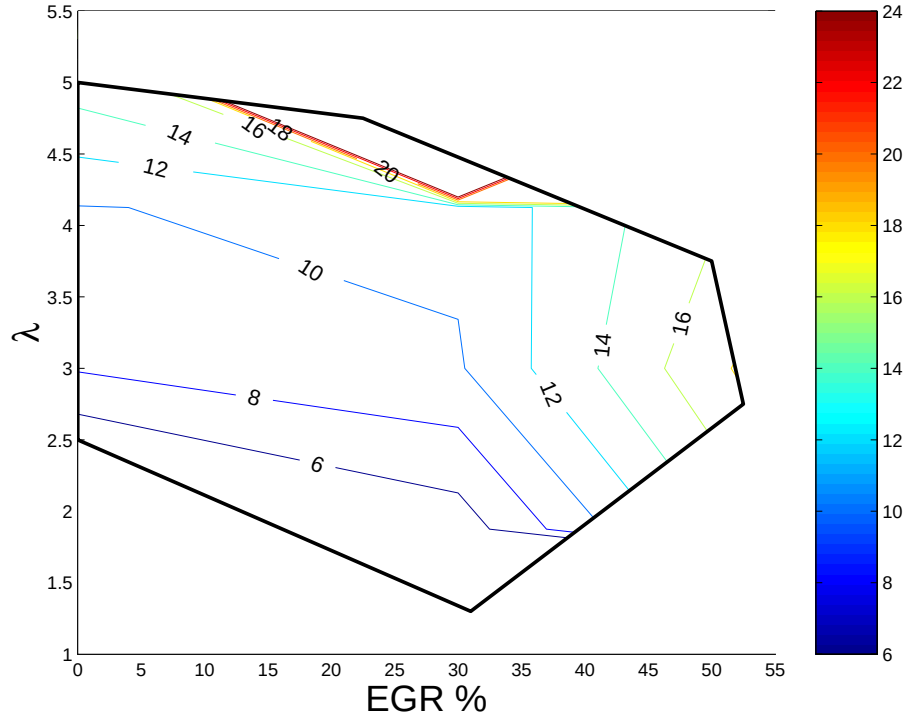

(a) Combustion duration prediction

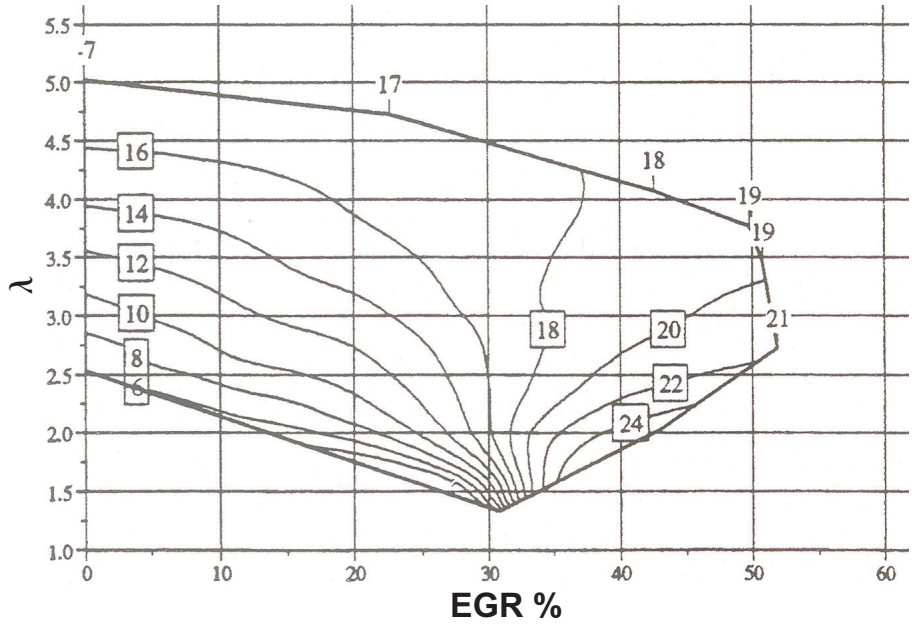

(b) Combustion duration measurements

Figure 11: *Combustion duration (CAD) as a function of air/fuel ratio and EGR.*

The charts for CO, HC and NO_x emissions are given in Figures 12 to 14. The CO emissions depicted in Figure 12, increased with increasing air dilution. Near the partial burn boundary, maximum CO emissions were observed due to the incomplete oxidation of the air-fuel charge. In this region the CO emissions were reliably predicted by the PDF-based full cycle model. At high loads, the CO emissions reduced with better oxidation of the air-fuel mixture.

The NO_x emissions as shown in Figure 13 were the highest in the high load limit, due to the higher in-cylinder temperatures. In the proximity of the partial burn boundary, with very low in-cylinder temperatures, the NO_x emissions were predicted lower than those observed experimentally.

Maximum specific unburned hydrocarbon emissions (Figure 14) were obtained near the partial burn boundary where the air dilution was the highest. This is due to the low overall combustion temperatures preventing the complete oxidation in this region. Minimum HC emissions were observed with high load limits. The HC emissions in the proximity of partial burn region were predicted accurately by the model as compared to the measurements. However, in the high load region of the window the emissions were under-predicted by 50%.

It should be noted that the wall temperature changes with varying in-cylinder temperature over the operating range. Additionally, as discussed in section **??**, the CO and HC emissions are sensitive to the wall temperature. A fixed temperature of 450 K was used to simulate the engine over the entire operating range. Thus, the prediction could be improved by accounting for a better estimation of wall temperature distribution.

In summary, the combustion parameters, emissions and the engine parameters are predicted well by the model over the entire operating range. In consequence, for developing an operating window for the HCCI engine, the SRM-PI based engine cycle simulator offers a reliable and time as well as cost effective tool.

Following the rigorous model validation and development of the operating window of the engine, model prediction of the misfire phenomenon is presented in the next section.

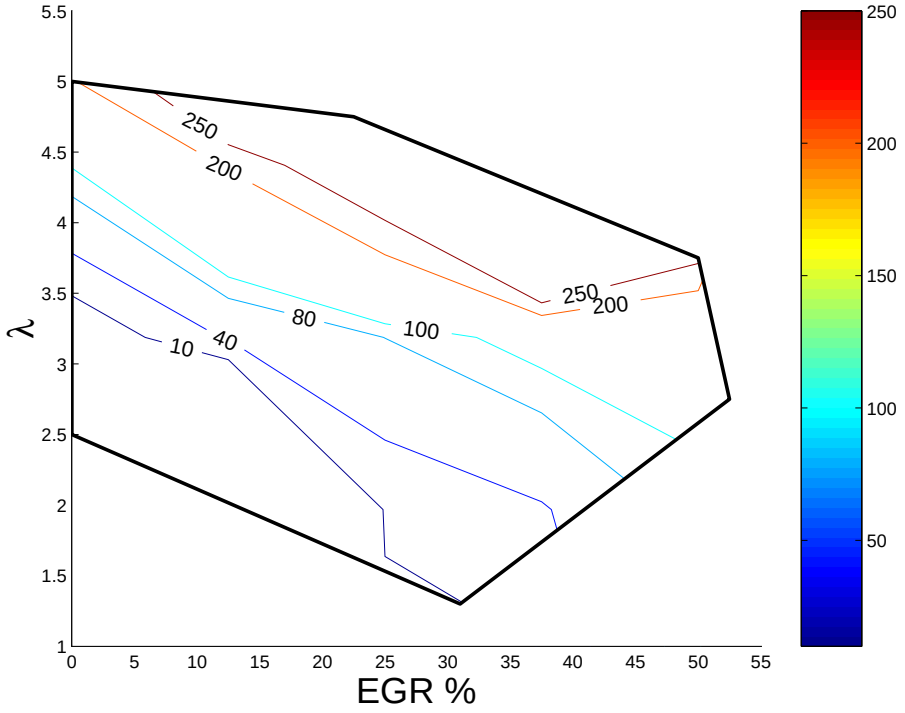

(a) CO emissions prediction

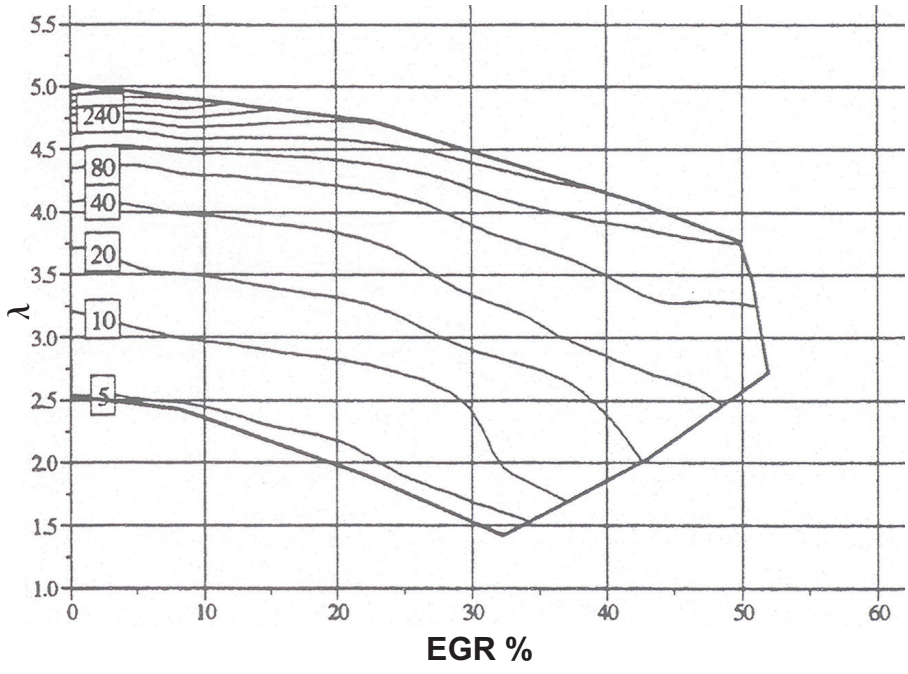

(b) CO emissions measurements

Figure 12: *CO emissions (g/kWh) as a function of air/fuel ratio and EGR.*

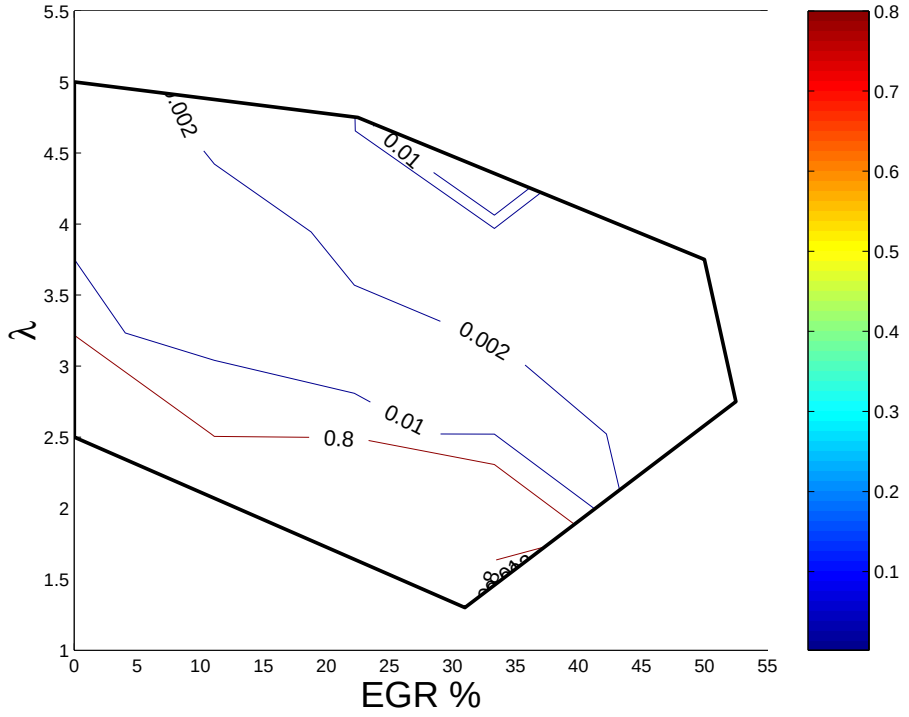

(a) NO_x emissions prediction

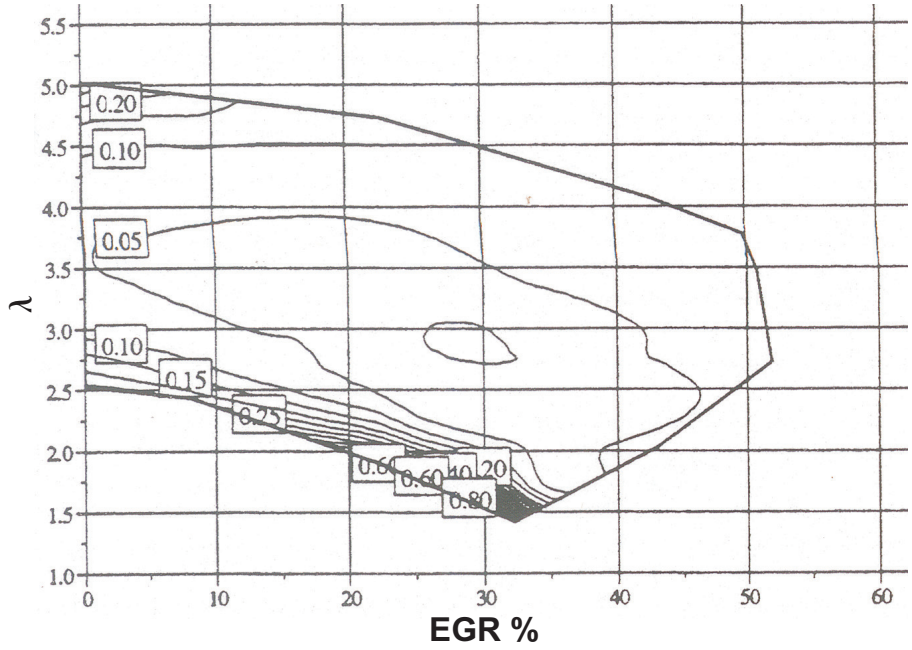

(b) NO_x emissions measurements

Figure 13: *NO_x emissions (g/kWh) as a function of air/fuel ratio and EGR.*

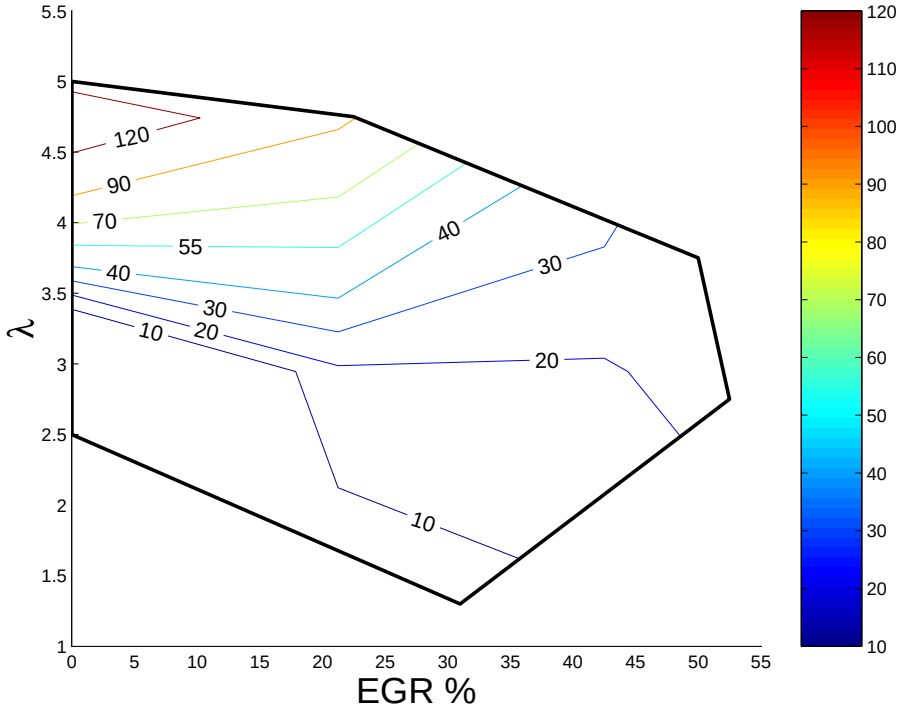

(a) HC emissions prediction

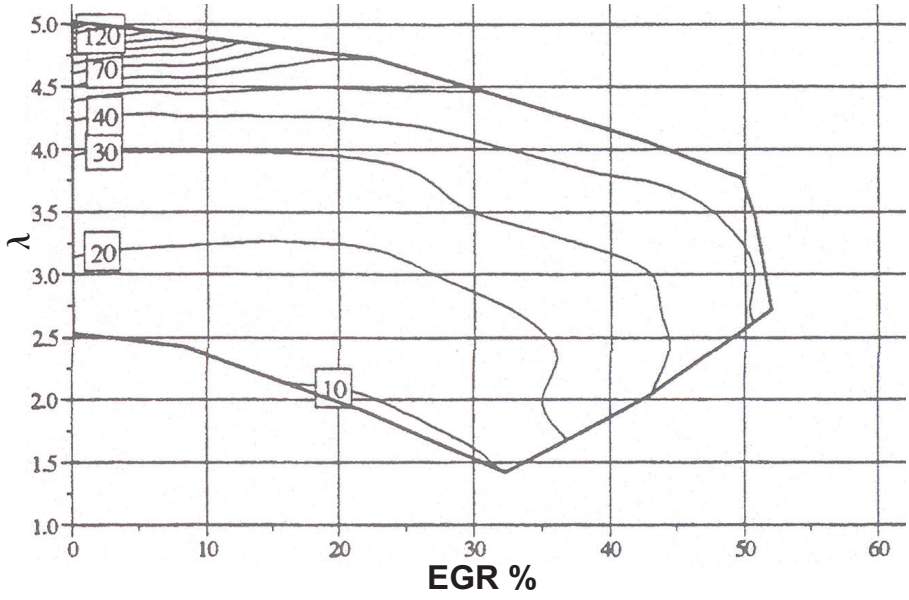

(b) HC emissions measurements

Figure 14: *HC emissions (g/kWh) as a function of air/fuel ratio and EGR.*

6 Misfire prediction

Misfire occurs due to intolerable amounts of EGR in the cylinder. The points corresponding to $\lambda = 3.0, EGR = 52\%$ and $\lambda = 3.7, EGR = 50\%$ (Figure 5) are located closest to the region bounded by misfire occurrence. For such points, the simulation set-up comprising 50 + 4 + 2 cycles would be insufficient to capture the effect of misfire. Hence, in addition to the 50 uncoupled and 4 coupled cycles with homogeneous reactor based model, 10 SRM-PI based coupled cycles were used. All the other parameters were left unchanged. The ignition crank angle degree (CAD) obtained with this method for a point corresponding to $\lambda = 3.0, EGR = 52\%$ is shown in Figure 15. Ignition CAD is the time at which 10% of mass is burnt. The effect of misfire is demonstrated by the high cycle to cycle variation in CAD. This effect is also evident in Figure 16(a) which depicts the fluctuations in the in-cylinder temperature relative to the cycles.

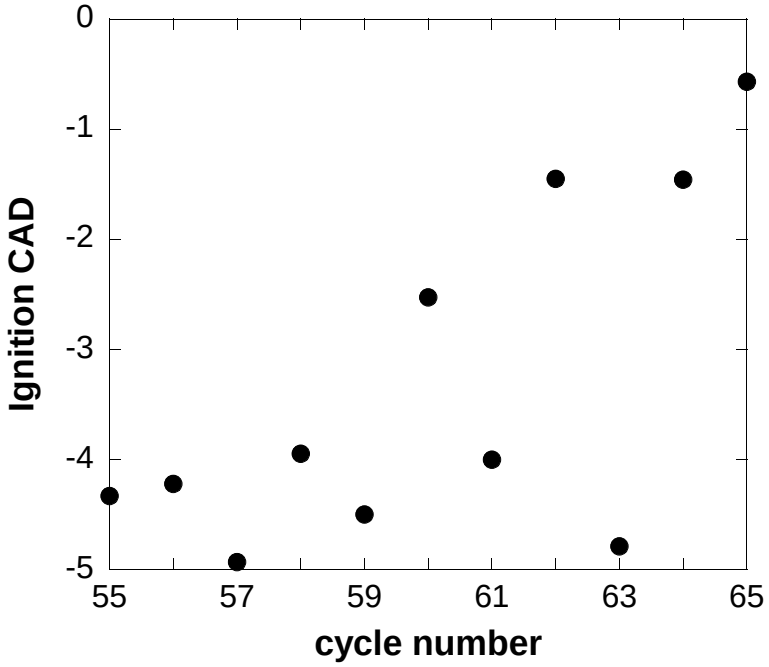

Figure 15: *Ignition CAD variation at the point,* $\lambda = 3.0, EGR = 52\%$.

For example, during cycle 60, the inlet charge failed to burn resulting in a misfire. For the subsequent cycle 61, although the temperature at IVC was 10 K lower than that for cycle 60 (Figure 16(b)), with 50% EGR percentage being recycled back, the large amount of unburnt fuel from the cycle 60 was introduced in the next cycle. This rich fuel burnt instantaneously and vigorously resulting in a high peak temperature in cycle 61. The ignition crank angle degree was delayed for cycle 61 as the air-fuel charge failed to burn, whereas, the ignition was advanced for the subsequent cycle.

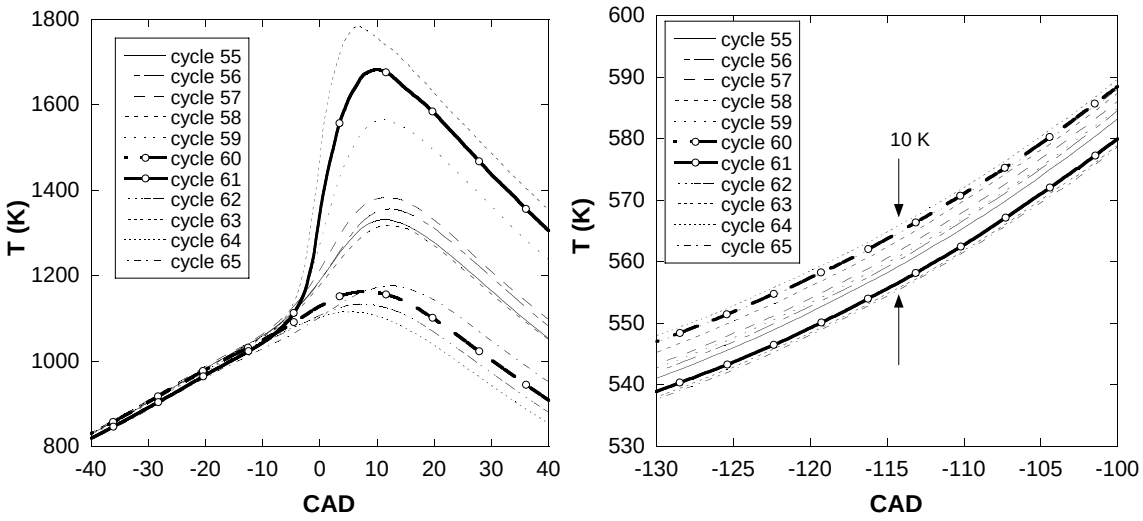

(a) In-cylinder temperature variation

(b) In-cylinder temperature during compression

Figure 16: *In-cylinder temperature as a function of cycle number, at a point corresponding to* $\lambda = 3.0, EGR = 52\%$.

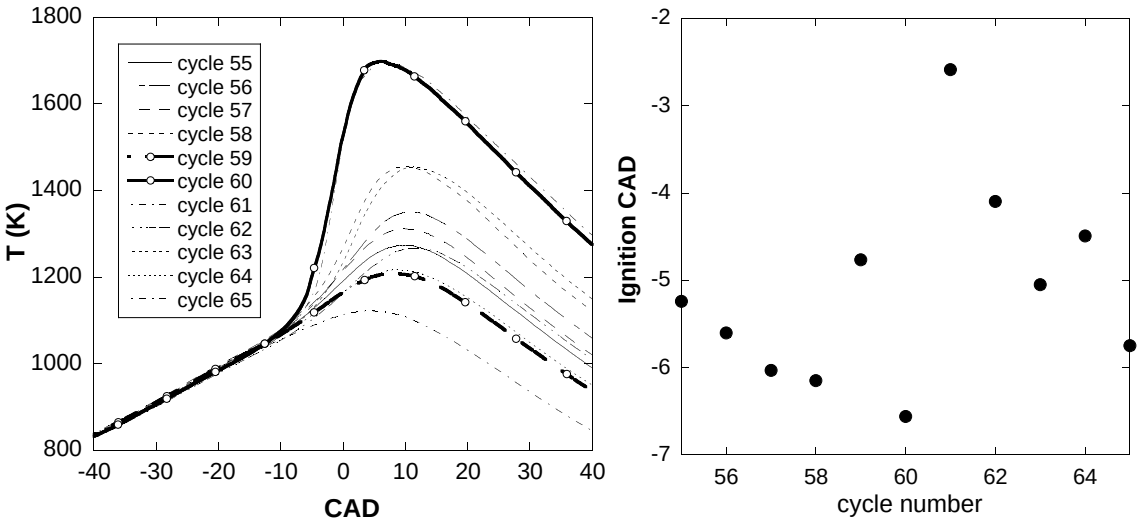

(a) In-cylinder temperature variation

(b) Ignition CAD variation

Figure 17: *Cyclic variation in the in-cylinder temperature and ignition-CAD at a point corresponding to* $\lambda = 3.7, EGR = 50\%$.

Similar effect was observed for the point corresponding to $\lambda = 3.7, EGR = 50\%$ and is shown in Figure 17. This effect of cyclic variation on combustion was observed by Koopmans and Backlund (2002) in their experimental study.

Comparing this behaviour with the in-cylinder temperature evolution (with respect to the number of cycles) at a point corresponding to $\lambda = 3.5, EGR = 1\%$, a very low cycle-to-cycle variation was observed as expected (Figure 18).

The CO and HC emissions are sensitive to the cyclic variations in temperature. Hence, in accordance with the experimental procedures, an average over 10 cycles was used to evaluate the emissions for the points near misfire boundary.

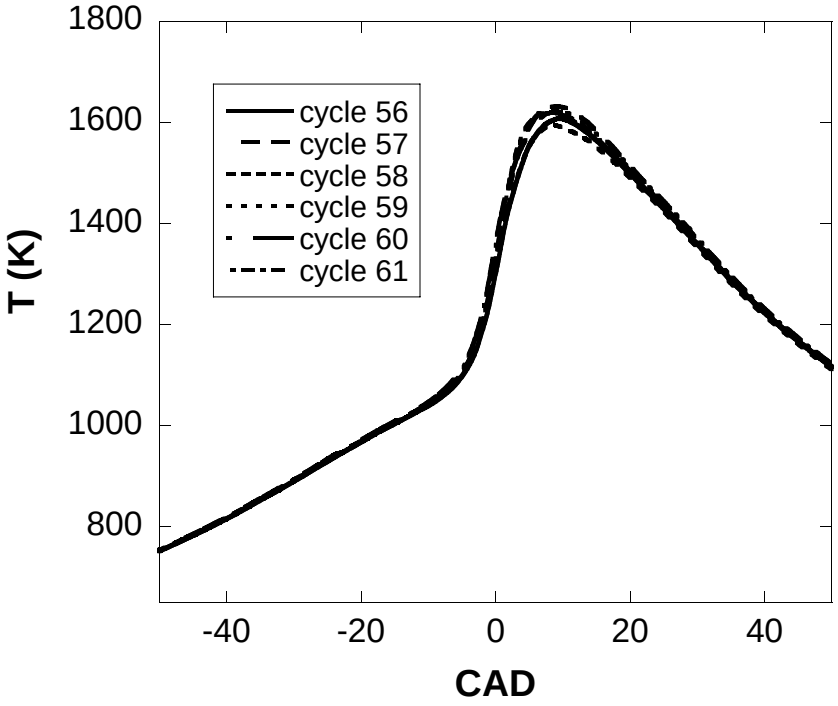

Figure 18: *Low cyclic variation at point,* $\lambda = 3.5, EGR = 1\%$.

7 Control options

In this section two control options, namely trapping residual burnt gas by variable valve timing and intake charge heating have been investigated. For this, the fuel flow rate (7.5 mg/cycle) and other model parameters discussed in section 4, are kept constant.

Recently, these two control techniques have been compared for a direct injection HCCI engine (Koopmans et al.; 2004). There is however, a substantial difference since port injection injects fuel into fresh air, while during direct injection, the fuel mixes with residuals trapped during negative valve overlap. As a consequence Koopmans et al. (2004) focussed on studying the distribution of temperature, residual burnt fraction and equivalence ratio for the aforementioned techniques, while no consideration was given to the combustion parameters and emissions.

7.1 Valve timing-residual trapping technique

External EGR works well due to its simplicity but its thermal effect is limited due to the heat loss in the EGR system and slow response during transient time. In comparison retaining the exhaust residual gas in the cylinder via cam phasing can avoid many of the system issues encountered with the external EGR approach (Zhao et al.; 2003). Such trapping of residual gas in a four-stroke HCCI engine emulates the in-cylinder conditions of a two-stroke engine. The thermal energy of the trapped residual gas enhances auto-ignition (Willand et al.; 1998). Furthermore, this approach does not need high compression ratios or a heater to increase the charge temperature, thus enabling a switching over from SI to HCCI mode of operation. However, with the engine operated unthrottled and at very low loads there is not enough thermal energy within the exhaust gas to achieve auto-ignition (Onishi et al.; 1979).

The residual burned fraction is a technique exploited by many researchers to control combustion phasing. Kontarakis et al. (2000) modified the conventional valve timing of a port injected four-stroke SI engine (CR=10.3:1) to late IVO and early EVC, and demonstrated the induction of HCCI without intake air heating or very high compression ratios. HCCI operation was observed to produce low NO_x and high unburned HC emissions at $\lambda = 1$, and fuel consumption during HCCI was comparable with that during SI operation. The tappet height reduction to allow adjustment of valve opening periods and thereby the gap between the tappet and cam is undesirable for production engines due to durability issues and excessive noise in the valve train mechanism, and hence a need for implementing fully variable valve lift and timing mechanism was emphasized.

Lavy et al. (2000) studied two-stroke and four-stroke configurations and concluded that varying the residual gas rate is the main factor for convergence towards favourable 2-stroke conditions for auto-ignition. Using mechanical valve actuation based on a camshaft with removable cams, the exhaust valve timing was observed to expand the operating range of auto-ignition towards higher load conditions. Two fundamentally different methods for controlled auto-ignition comprising of a more sophisticated active valve train that alleviate the necessity of intake charge heating and enable probing cam-less engines, have been introduced by (Law et al.; 2001). First, a sequential method employed trapping of residual burned fraction by late closing of the exhaust valve and re-compressing the fresh intake charge with the residual burned fraction. In the second method, at the commencement of the induction stroke both inlet and exhaust valves were opened simultaneously thus drawing fresh charge as well as exhaust gases into the cylinder (re-breathing). With both the methods the pressure profiles obtained were similar and the amount of residual burned fraction determined the combustion initiation point. In case of the re-breathing method, significant heat loss at the exhaust port resulted in poorer preservation of the thermal energy compared to that in the re-compression method. In another study HCCI combustion was achieved with residual gas trapping (46-65%) using variable cam timing (Li et al.; 2001). The upper and lower limits for stable HCCI operation were

attributed to the gas exchange restriction at high loads and misfire at low loads respectively. Use of EGR and supercharging to extend the limit on the upper side, whereas at the lower end, a need for other ways of raising the in-cylinder temperature was pointed out.

Koopmans and Denbratt (2001) observed experimentally the transition from SI to HCCI combustion on increasing the amount of residual gas fraction by increasing the negative valve overlap of the EVC with IVO symmetrically. With equivalence ratios maintained in the range 1 and 0.77, HCCI mode offered clear benefit in terms of reduction in CO and NO_x emissions and fuel consumption, compared to the SI operation. Koopmans and Backlund (2002) have utilized a four-stroke, naturally aspirated, camless HCCI engine with early EVC while predicting cyclic variations.

Sensitivities of exhaust and intake valve timings on the mass exhaled and inhaled have been investigated by Xu et al. (2002). They implemented a single zone based full cycle model to simulate a PRF fuelled HCCI combustion. The EVC timing was observed to strongly influence the mass flow rates at intake and exhaust and hence the load. Whereas, IVO timing affected pumping losses significantly. The low pumping loss achievable due to gas exchange was beneficial in terms of fuel economy improvement at part load. In the same work, moderate intake air heating was observed to reduce the requirement of the EGR and thus widen the operating range at light load.

The effect of increased trapped residual with negative valve overlap on HCCI combustion has been systematically simulated by Babajimopoulos et al. (2002). They implemented a segregated sequential CFD-driven full cycle modelling approach to simulate a port injected, natural gas fuelled HCCI combustion. With increase in the negative valve overlap, a large amount of residual burned fraction (up to 66%) was trapped in the cylinder and less fresh charge was introduced. The hot trapped fraction resulted in an increase in the temperature just before EVO. In addition, the trapped residual burned gas contained appreciable oxygen thus lowering the equivalence ratio. Due to these conditions, the onset of combustion was advanced, but the peak temperature was lower due to the low equivalence ratio (dilution effect). However, in order to save the computational expense, a computational grid inadequate to account for boundary layer and crevice was used. This is probably the reason, for not including the effect of variable valve actuation on emissions in their study. Furthermore, a need to account for the inhomogeneities in composition and temperature was emphasized and mixing has been argued to be a crucial parameter in modelling HCCI combustion especially with a high residual burned fraction. In an extension to this study, Babajimopoulos et al. (2003) employed inhomogeneity in composition, in addition to the inhomogeneity in temperature. An interesting result for a high residual burnt fraction trapping (42%), showed that for a high average in-cylinder temperature condition the effect of temperature inhomogeneity nullified that of composition inhomogeneity. However, in the marginal combustion case (ignition timing delayed and combustion duration extended), the pressure profile predicted was different than the equivalent prediction in their previous work.

Recently, Persson et al. (2004) investigated the effect of the intake temperature on HCCI operation with negative valve overlap in a four-stroke port injected engine. At high load condition, the change in the intake temperature was observed to have only a modest impact, as the temperature of the trapped residuals was much higher than the intake temperature.

In the present study, the PDF based full cycle model was applied to investigate the effect of trapped residual burned fraction using late IVO and early EVC. The EGR valve was completely closed to study the effect of residual burned fraction (RBF) alone. The inlet and exhaust valve timings are given in Table 3.

Table 3: *Inlet and exhaust valve timings.*

Events	**IVO (°)**	**IVC (°)**	**EVO (°)**	**EVC (°)**	**RBF (%)**
VT1	352	576.56	137	366.53	18.9
VT2	382	576.56	137	336.53	33.7
VT3	412	576.56	137	306.53	46.0
VT4	442	576.56	137	276.53	54.6

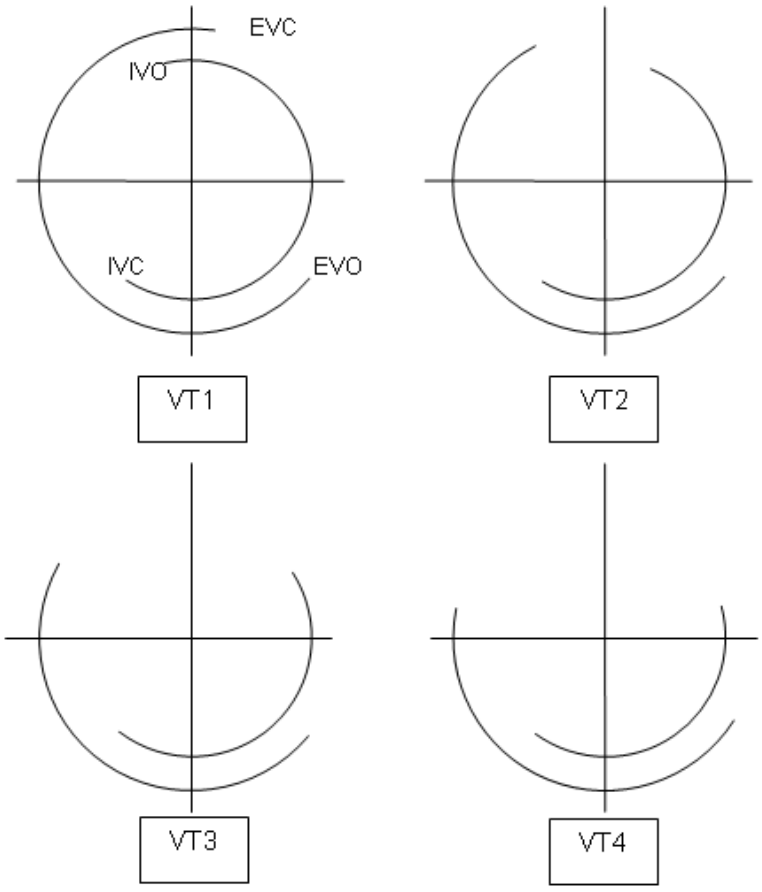

Figure 19: *Valve timings*

The valve timing events have been depicted in the Figure 19. Increasing the negative valve overlap led to larger amount of trapped residual burned fractions in the engine cylinder. In this study, the fuel flow was maintained constant at 7.5 mg/cycle. Thus with increasing residual burned fractions, the amount of air is reduced i.e, the air-fuel ratio λ decreases as the overlap is increased. Hence the dilution effect of EGR is overshadowed by the constant fuel flow rate and the increased temperature of the residuals.

Figure 20 depicts the in-cylinder temperature variation for various valve timing events. The hot trapped residual fraction advanced the auto-ignition of the air-fuel charge leading to higher peak temperatures (decrease in λ). The second hump observed in the temperature profile following the gas exchange process is caused by the re-compression of the residual burned gas mass fraction in this period.

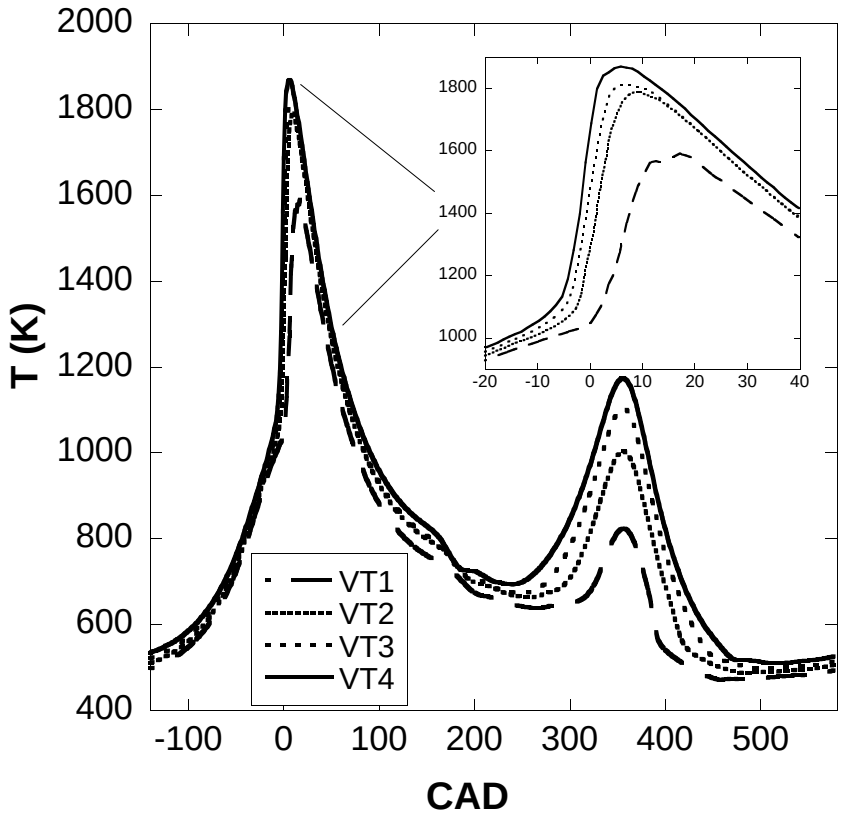

Figure 20: *Effect of RBF on in-cylinder temperature.*

As observed in Figure 21, the intake pressure and the pressure during compression was the same for all the four valve timing events.

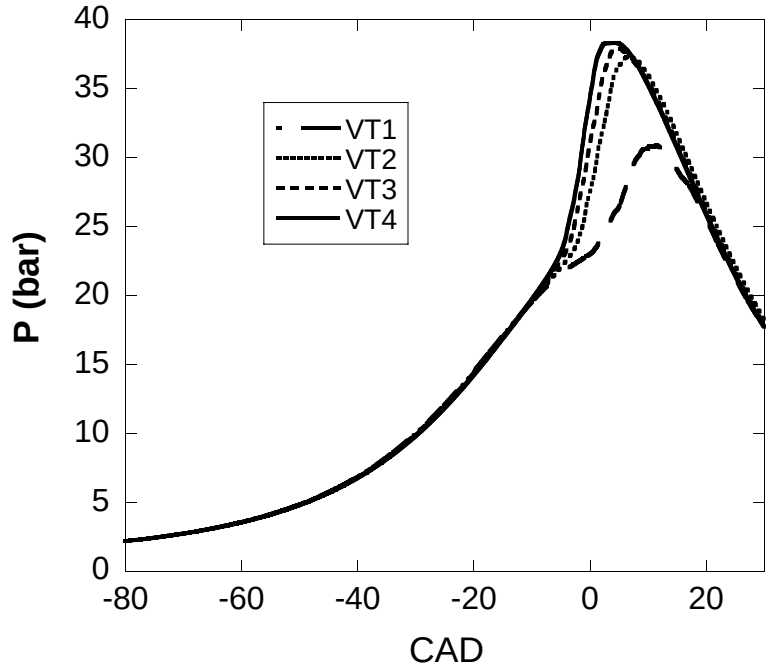

Figure 21: *Effect of RBF on in-cylinder pressure.*

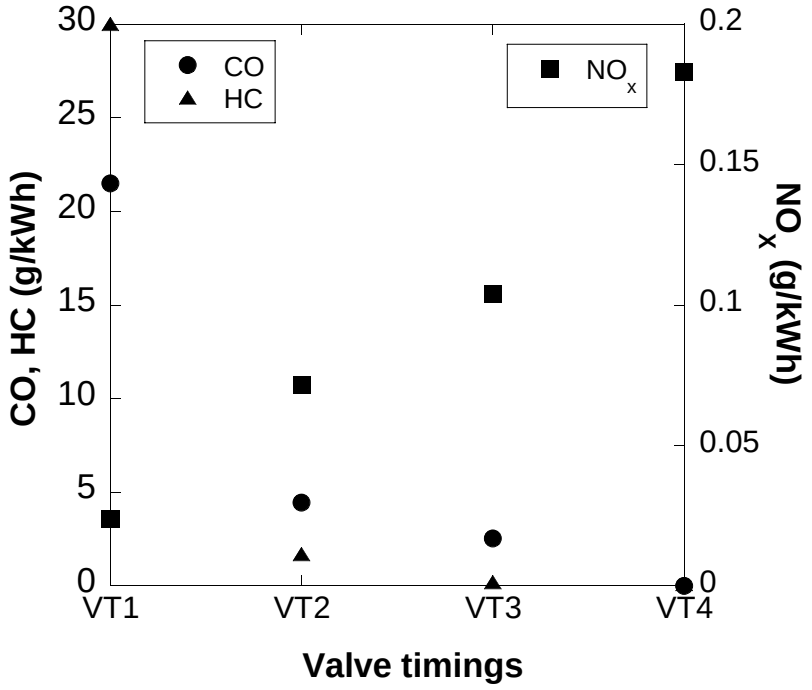

Figure 22: *Effect of RBF on CO, HC and NO_x emissions.*

The CO and HC emissions reduced with increase in the in-cylinder temperatures, whereas the temperature sensitive NO_x emissions increased as shown in Figure 22).

7.2 Intake temperature variation

The inlet charge temperature, i.e., the charge conditions at IVC is a convenient and efficient way to control the auto-ignition timing. This approach combined with variable compression ratio has been widely used for earlier four-stroke HCCI development on account of its effectiveness and practicality in controlling combustion phasing (Najt and Foster; 1983; Thring; 1989; Christensen et al.; 1998). This method is the most widely applied HCCI control approach as the combustion timing is very sensitive to intake charge temperature (Christensen and Johansson; 2002; Stanglmaier and Roberts; 1999; Olsson et al.; 2000). The high intake temperature speeds up the onset of low-temperature (cool flame) chemistry, in turn reducing the main stage ignition delay. In addition at low loads, with the intake temperature strongly influencing the CO emissions, Olsson et al. (2001) have emphasized the need of intake charge heating to control the CO and HC emissions.

However, this technique also has some drawbacks: For multi-cylinder engines, this control-option requires a very large power supply. Second, the thermal inertia of the cylinder wall and the intake manifold makes it difficult to change the inlet air temperature from cycle to cycle. Furthermore in case of vehicle applications, unless the exhaust gas energy is utilized to provide the required heat, this method is considered as impractical (Xu et al.; 2002).

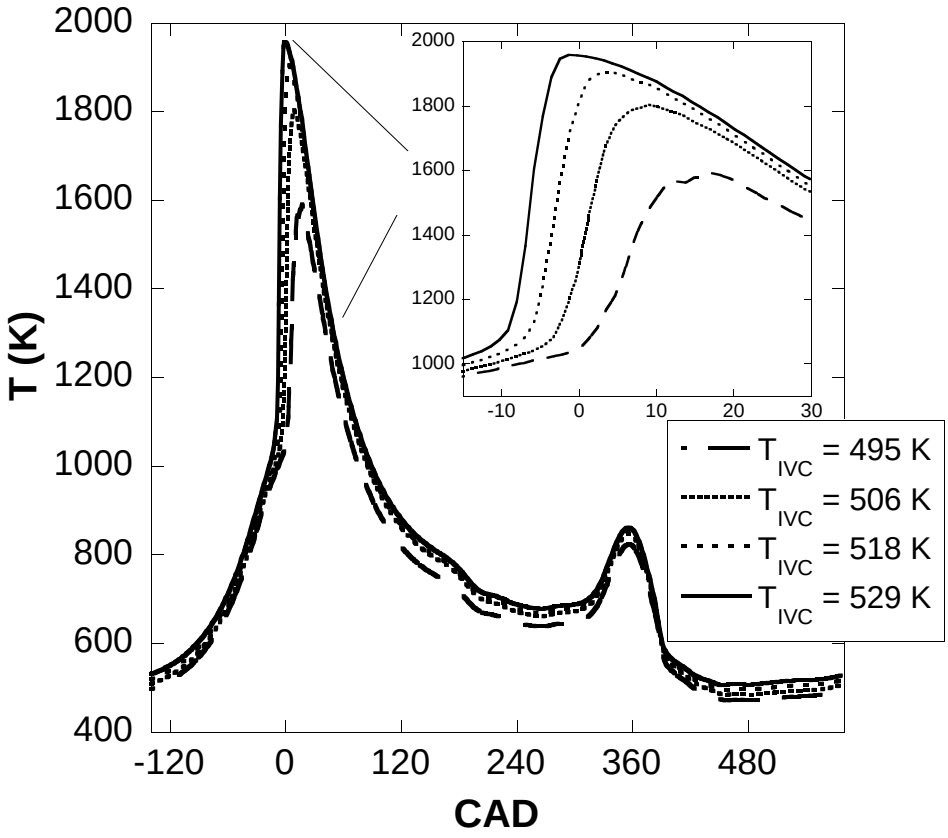

Figure 23: *Effect of intake temperature (at IVC) on in-cylinder temperature.*

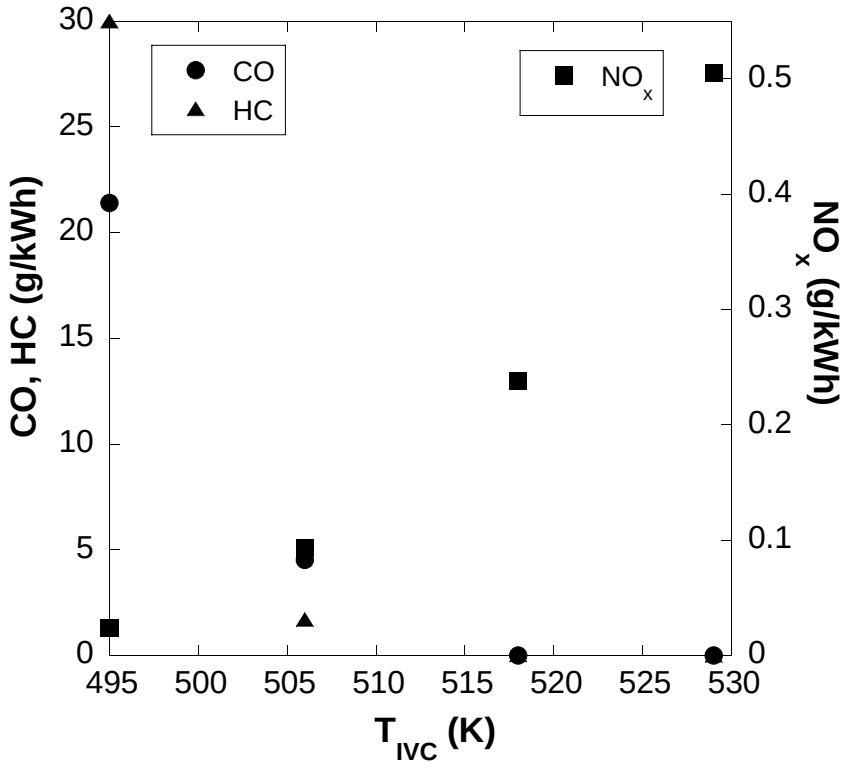

Figure 24: *Effect of intake temperature (at IVC) on CO, HC and NO_x emissions.*

In this section, the original valve timing (VT1) given in Table 1 was used, and the temperature at IVC was raised in steps of approximately 11 K. As expected, an increase in the intake temperature enhanced the auto-ignition, increased the peak temperatures and reduced the CO and HC emissions.

Comparing both the control options, the auto-ignition timing as well as the peak temperature is more sensitive to the intake charge heating than the residual burnt trapping technique.

The homogeneous initial condition (section 3) for the temperature and composition of the particles may be justified by the following reasons:

With a constant fuel flow rate of 7.5 mg/cycle and the heater temperature at 593 K, high in-cylinder temperatures were observed with negative valve overlap. As demonstrated by Babajimopoulos et al. (2003), for an appreciable amount of residual burnt fraction trapped and high in-cylinder temperature condition the effect of temperature inhomogeneity nullifies that of composition inhomogeneity. In the present study, fluctuations are induced in the temperature distribution of the ensemble, and the mixing model accounts for inhomogeneities in the composition as well as temperature. Hence, considering a homogeneous initial condition for composition and temperature of the stochastic particles at IVC is justified.

With variable valve timing, the re-compression of the trapped residual gas, increases the temperature at exhaust (Figure 20). This effect is absent in the case of intake

charge heating. Stanglmaier et al. (2001) have cautioned about the potential problem of low exhaust temperatures of an HCCI engine while using oxidation catalysts for CO and HC emissions reduction. The high exhaust temperatures obtained with negative valve overlap have the potential to enable the use of a conventional oxidation catalyst for reducing the CO and HC emissions, in agreement with the results demonstrated experimentally elsewhere (Kontarakis et al.; 2000; Olsson et al.; 2001; Persson et al.; 2004). However, at very light loads, the temperature rise due to trapped residual gas is not high enough to trigger auto-ignition. In such situations, a combination of the two techniques i.e., using intake heating with negative valve overlap could be helpful.

With both the techniques, the increase in the in-cylinder temperatures reduced the HC and CO emissions and increased the NO_x emissions, in agreement with the experimental observations Van Blarigan et al. (1998); Christensen et al. (1998).

8 Conclusions

HCCI operation in a PRF-fuelled, single cylinder, four-stroke HCCI engine with exhaust gas recirculation was modelled using the PDF based engine cycle model. The model predictions for the in-cylinder temperature and HC emissions were validated against the measurements for a base case, and showed a satisfactory agreement.

Furthermore, the model was implemented to develop an operating window for various combustion and emission parameters as a function of the amount of EGR and the air/fuel ratio. The model predictions over the entire operating range for all the parameters investigated, were compared with the experimental results. This rigorous validation test, and a reasonably good agreement between the trends as well as the magnitudes of predicted and experimental quantities, suggested the robustness of the model for simulating the HCCI operation. The three boundaries of a stable HCCI operation, namely the partial burn, knock, and misfire were reliably predicted by the model. The occurrence of knock was described in terms of the excessively rapid rate of pressure rise. The partial burn boundary was denoted by a very low IMEP and high CO and HC emissions. The model provides an insight into misfire phenomenon and a possible way it could be accounted for while modelling HCCI operation. The misfire was demonstrated by considering a multiple cycle simulation where the intake charge failed to burn during some of the cycles.

Thus, the integrated PDF based model serves as an efficient tool to construct and understand the operating window for HCCI engines. Such operating windows can be developed for various fuels and compared, while studying the influence of the type of fuel on HCCI characteristics. With the inclusion of detailed chemistry, the PDf based model is applicable over the entire range of operating conditions, in comparison to the reduced mechanisms which are valid only for a limited range of thermodynamic conditions. Additionally, an operating window is useful for estimating the effect of various control parameters on the expansion of the operating window to high loads.

Finally, two control options, i.e., residual burnt fraction trapping by variable valve timing and intake charge heating were investigated. The usefulness of negative valve overlap in obtaining higher exhaust gas temperatures, thereby enabling the use of conventional CO and HC removal oxidation catalysts was demonstrated. However, the need for a combination of the two control techniques at light loads was pointed out. As a result, a possible implementation strategy for HCCI engine production was identified: at very low loads intake temperature heating with some residual gas trapping; at low to medium loads residual gas trapping alone; and at high loads SI operation, could enable a stable engine operation over the entire operating range. Such a hybrid operation with SI is possible as the intake temperature and residual burnt gas ensure that the in-cylinder conditions are right for auto-ignition without any need for increasing the compression ratio, thus facilitating the hybridization with a low compression ratio SI mode.

9 Acknowledgements

The authors would like to thank Kayiu Man at Brunel University, and Steven Liput at the University of Cambridge for their help in representing the experimental set up on the 1-D code interface. The authors are grateful to the Cambridge Commonwealth Trust, and the Centre for Scientific Enterprise Ltd. for their financial support.

References

Aichlmayr, H. T., Kittelson, D. B. and Zachariah, M. R. (2002). Miniature free-piston homogeneous charge compression ignition engine-compressor concept-partii: Modeling hcci combustion in small scales with detailed homogeneous gas phase chemical kinetics, *Chem. Engng. Sci.* **57**: 4173–4186.

Babajimopoulos, A., Assanis, D. N. and Fiveland, S. (2002). Controlled combustion in an ic engine with a fully variable valve train, *SAE Paper 2002-01-2829*.

Babajimopoulos, A., Lavoie, G. A. and Assanis, D. N. (2003). Modeling hcci combustion with high levels of residual gas fraction - a comparison of two vva strategies, *SAE Paper 2003-01-3220*.

Bhave, A. N., Balthasar, M., Mauss, F. and Kraft, M. (2004a). Analysis of a natural gas fuelled hcci engine with exhaust gas recirculation using a stochastic reactor model, *Int. J. Engine Res.*

Bhave, A. N., Kraft, M., Montorsi, L. and Mauss, F. (2004b). Modelling a dual fuelled multi-cylinder hcci engine using a pdf based engine cycle simulator, *SAE Paper 2004-01-0561*.

Chen, Z., Konno, M. and Goto, S. (2001). Study on homogeneous premixed charge ci engine fueled with lpg, *JSAE Review* **22**: 265–270.

Christensen, M. (2002). *PhD Thesis: HCCI Combustion - Engine Operation and Emission Characteristics*, Department of Heat and Power Engineering, Lund Institute of Technology.

Christensen, M. and Johansson, B. (2002). The effect of in-cylinder flow and turbulence on hcci operation, *SAE Paper 2002-01-2864*.

Christensen, M., Johansson, B., Amneus, P. and Mauss, F. (1998). Supercharged homogeneous charge compression ignition, *SAE Paper 980787*.

Gentili, R. and Frigo, S. (2000). Further insight on atac and gdi combination in two-stroke engines, *SAE Paper 2000-01-0897*.

Kontarakis, G., Collings, N. and Ma, T. (2000). Demonstration of hcci using a single cylinder four-stroke si engine with modified valve timing, *SAE Paper 2000-01-2870*.

Koopmans, L. and Backlund, O. (2002). Cycle to cycle variations: Their influence on cycle resolved gas temperature and unbruned hydrocarbons from a camless gasoline compression ignition engine, *SAE Paper 2002-01-0110*.

Koopmans, L. and Denbratt, I. (2001). A four stroke camless engine operated in homogeneous charge compression ignition mode with commercial gasoline compression ignition engine, *SAE Paper 2001-01-3610*.

Koopmans, L., Wallesten, J., Ogink, R. and Denbratt, I. (2004). Location of the first auto-ignition sites for two hcci systems in a direct ignition engine, *SAE Paper 2004-01-0564*.

Lavy, J., Dabadie, J. C., Angelberger, C., Duret, P., Willand, J., Juretzka, A., Schäflein, J., Ma, T., Lendresse, Y., Satre, A., Schulz, C., Krämer, H., Zhao, H. and Damiano, L. (2000). Innovative ultra-low nox controlled auto-ignition combustion process for gasoline engines: the 4 space project, *SAE Paper 2000-01-1837*.

Law, D., Kemp, D., Kirkpatrick, G. and Copland, T. (2001). Controlled combustion in an ic engine with a fully variable valve train, *SAE Paper 2000-01-0251*.

Li, J., Zhao, H., Ladommatos, N. and Ma, T. (2001). Research and development of controlled auto-ignition (cai) combustion in a 4-stroke multi-cylinder gasoline engine, *SAE Paper 2001-01-3608*.

Najt, P. and Foster, D. E. (1983). Compression ignited homogeneous charge combustion, *SAE Paper 830264*.

Oakley, A. (2001). *PhD Thesis: Experimental Investigations on Controlled AutoIgnition Combustion in a Four Stroke Gasoline Engine*, Department of Mechanical Engineering, Brunel University.

Oakley, A., Zhao, H., Ladommatos, N. and Ma, T. (2001). Dillution effects on the controlled auto-ignition (cai) combustion of hydrocarbon and alcohol fuels, *SAE Paper 2001-01-3606*.

Olsson, J. O., Erlandsson, O. and Johansson, B. (2000). Experiments and simulation of a six-cylinder homogeneous charge compression ignition (hcci) engine, *SAE Paper 2000-01-2867*.

Olsson, J. O., Tunestål, P., Haraldsson, G. and Johansson, B. (2001). A turbocharged dual fuel hcci engine, *SAE Paper 2001-01-1896*.

Onishi, S., Jo, S. H., Shoda, K., Jo, P. D. and Kato, S. (1979). Active thermo atmospheric combustion (atac) - a new combustion process for internal combustion engines, *SAE Paper 790501*.

Persson, H., Agrell, M., Olsson, J., Johansson, B. and Ström, H. (2004). The effect of intake temoerature on hcci operation using negative valve overlap, *SAE Paper 2004-01-0944*.

Smith, J. R., Aceves, S. M., Westbrook, C. and W., P. (1997). Modeling of homogeneous charge compression ignition (hcci) of methane, *ASME 97-ICE-68*.

Stanglmaier, R. H. and Roberts, C. E. (1999). Homogeneous charge compression ignition (hcci): Benefits, compromises and future engine applications, *SAE Paper 1999-01-3682*.

Stanglmaier, R. H., Ryan III, T. W. and Souder, J. S. (2001). Homogeneous charge compression ignition with a free piston: A new approach to ideal otto cycle performance, *SAE Paper 2001-01-1897*.

Thring, R. H. (1989). Homogeneous charge compression ignition (hcci) engines, *SAE Paper 892068*.

Van Blarigan, P., Paradiso, N. and Goldsborough, S. (1998). Homogeneous charge compression ignition with a free piston: A new approach to ideal otto cycle performance, *SAE Paper 982484*.

Willand, J., Nieberding, R. G., Vent, G. and Enderle, C. (1998). The knocking syndrome - its cure and its potential, *SAE Paper 982483*.

Xu, H., Fu, H., Williams, H. and Shilling, I. (2002). Modelling study of combustion and gas exchange in a hcci (cai) engine, *SAE Paper 2002-01-0114*.

Zhao, F., Asmus, T. W., Assanis, D. N., Dec, J. E., Eng, J. A. and Najt, P. M. (2003). *Homogeneous Charge Compression Ignition (HCCI) Engines: Key Research and Development Issues*, 1st edn, SAE Inc., Canada, pp. 1–658.

Zhao, H., Li, J., Ma, T. and Ladommatos, N. (2002). Performance and analysis of a 4-stroke multi-cylinder gasoline engine with cai combustion, *SAE Paper 2002-01-0420*.